

RADIATION FROM COLLAPSING RELATIVISTIC STARS. I. LINEARIZED ODD-PARITY RADIATION*

CHRISTOPHER T. CUNNINGHAM AND RICHARD H. PRICE

Department of Physics, University of Utah

AND

VINCENT MONCRIEF

Department of Physics, Yale University

Received 1977 December 16; accepted 1978 March 9

ABSTRACT

Wave equations are derived in terms of gauge-invariant amplitudes for odd-parity electromagnetic and gravitational perturbations of Oppenheimer-Snyder collapse. Numerical studies of the wave equations are presented, and it is shown that for the late stages of collapse (i) the radiation generated is insensitive to the dynamics of the stellar interiors, (ii) the radiation spectrum is dominated by radiation of quasi-normal frequencies, and (iii) l -pole fields fall off at very late times t in accordance with the predicted $t^{-(2l+2)}$ law.

Subject headings: gravitation — quantum mechanics — relativity — stars: collapsed

I. INTRODUCTION AND OUTLINE

This is the first in a series of papers in which we hope to provide a detailed study of radiation emitted in the late stages of gravitational collapse to a slowly rotating black hole. In the present paper we analyze electromagnetic and gravitational radiation due to odd-parity sources in a collapsing Oppenheimer-Snyder (1939) (homogeneous, pressureless) background. The sources and the fields they produce are treated as linearized perturbations. In subsequent papers we shall deal with (i) the even-parity problem, (ii) radiation which is second order in the source strengths, and (iii) applications to astrophysical systems.

The emphasis in this paper is on an understanding of the special features of radiation peculiar to the late stages of collapse. We shall show that this radiation is rather independent of the internal dynamics of the collapsing star and that the nature of the radiation is governed by the background Schwarzschild spacetime surrounding the collapsing star.

The concept of the "curvature potential" provides a useful way of viewing the influence of the strongly curved Schwarzschild spacetime near the event horizon. Multipole test fields (gravitational, electromagnetic, scalar) on a Schwarzschild background all obey equations of the form

$$\partial^2\psi/\partial t^2 - \partial^2\psi/\partial r_*^2 + V(r)\psi = 0, \quad (\text{I-1})$$

where r_* is the tortoise coordinate (Misner, Thorne, and Wheeler 1973) defined in terms of black hole mass M and Schwarzschild radius r as

$$r_* = r + 2M \ln(r/2M - 1) + \text{const.}, \quad (\text{I-2})$$

so that the horizon is at $r_* = -\infty$. (We use here and throughout this paper units in which $c = G = 1$.) At large r_* the potential $V(r)$ approaches the form of a centrifugal barrier, $l(l+1)/r^2$; but as $r_* \rightarrow -\infty$, the potential dies off very rapidly. The curvature potential thus has some of the characteristics of a potential barrier, and all effects of the exterior geometry can be understood in terms of this potential barrier.

The Oppenheimer-Snyder collapse provides an extremely simple model for the interior, and its simplicity suits our purposes here very well. To get some first ideas on the effect of slower collapses, in which pressure is important, we have also computed the emerging radiation from modified Oppenheimer-Snyder models for which the collapse may be made arbitrarily slow.

Simplicity is also part of the motivation for the choice of odd-parity perturbations, since they obey markedly simpler junction conditions at the star's surface than do even-parity perturbations. The odd-parity gravitational perturbations are generated by small-amplitude rotational motions in the star's fluid. The electromagnetic perturbations are generated by circulating currents in the collapsing star.

* Work supported in part by National Science Foundation grants PHY74-16311 at the University of Utah and PHY76-82353 at Yale University.

Even-parity perturbations, generated by deformations of the fluid or by separation of electric charges, will be considered in a later paper. Although the junction conditions are much different for even-parity than for odd-parity (particularly for the gravitational perturbations), preliminary calculations indicate that qualitative features of the emitted radiation will be similar in both cases.

The physical model underlying the computations is that of a static star which suddenly, at time $t = 0$, loses its pressure and begins an Oppenheimer-Snyder collapse. The initial conditions on the perturbation field are then that for $t < 0$ the star has a stationary external odd-parity gravitational or magnetic multipole. We should in principle also have to specify the nature of the source distribution and Cauchy data for the perturbation field inside the star, but for a particular choice of the nature of the stationary star prior to the onset of collapse (and, in the electromagnetic case, for a natural choice of the behavior of the sources) this turns out not to be necessary. The source distribution and interior Cauchy data then contain only two numbers which influence the exterior field, and these two numbers are uniquely fixed by the magnitude of the initial stationary perturbation and by the radius (in units of the star's mass) at which collapse begins.

Two features of the emerging radiation are particularly interesting: power-law tails and quasi-normal ringing. The tails are the last traces of the dying field at very late times and have been predicted (Price 1972), for an initially stationary multipole of order l , to fall off as $1/t^{2l+2}$. This falloff, as well as the predicted radial dependence of the tails, has been verified to considerable accuracy.

Quasi-normal modes are damped oscillating modes of the Schwarzschild geometry, characterized by a single complex frequency. Previous studies (see Thorne 1978 for a review) indicate that these modes play some role in determining the nature of the radiation in the neighborhood of a black hole. We find in fact that the radiation emitted from the late stages of collapse is dominated by quasi-normal ringing and that an understanding of the excitation of the quasi-normal modes is necessary to understand the generation of radiation.

The paper is organized as follows: Section II presents a description of odd-parity gravitational and electromagnetic perturbation fields using gauge-invariant quantities. The perturbations are found to obey simple hyperbolic partial differential equations. Numerical solutions of these wave equations are described in § III, in which results are given for the waveforms, the energies, and the spectra of the emitted radiation. In § IV two features of the numerical results are discussed. First, the behavior of the perturbation at very late times ("power-law tail") is shown to conform to the theoretical predictions (Price 1972). Second, quasi-normal ringing is shown to dominate the emitted radiation, and the mechanism of the excitation of the quasi-normal modes is considered.

II. PERTURBATION EQUATIONS AND JUNCTION CONDITIONS

a) Gravitational Perturbations

We adopt Regge-Wheeler (1957) (RW) notation and expand the perturbed interior line element in odd-parity, axisymmetric RW harmonics:

$$\begin{aligned} ds^2 = & -d\tau^2 + R^2(\tau)[d\chi^2 + \sin^2 \chi(d\theta^2 + \sin^2 \theta d\phi^2)] \\ & + 2\epsilon[h_0 \sin \theta \partial Y_{10}/\partial \theta] dt d\phi + 2\epsilon[h_1 \sin \theta \partial Y_{10}/\partial \theta] d\phi d(\sin \chi) \\ & + 2\epsilon[\frac{1}{2}h_2(\cos \theta \partial Y_{10}/\partial \theta - \sin \theta \partial^2 Y_{10}/\partial \theta^2)] d\theta d\phi. \end{aligned} \quad (\text{II-1})$$

It is straightforward to extend these considerations to nonaxisymmetric modes as well. We shall consider only the radiative modes with $l \geq 2$. In equation (II-1), $R(\tau)$ is the ($k = +1$) Friedman expansion factor given by

$$R(\tau) = (M/\sin^3 \chi_0)(1 + \cos \eta), \quad (\text{II-2a})$$

where

$$\tau = (M/\sin^3 \chi_0)(\eta + \sin \eta) \quad (\text{II-2b})$$

in which M is the total (unperturbed) mass and χ_0 is the (stellar) boundary value of χ .

The metric perturbations $h_{\mu\nu} = \partial g_{\mu\nu}/\partial \epsilon|_{\epsilon=0}$ are determined by the RW expansion function $(h_0, h_1, h_2)(\chi, \tau)$. In terms of these we define

$$q_1 \equiv h_1 + \frac{\sin^2 \chi}{2 \cos \chi} \frac{\partial}{\partial \chi} \left(\frac{h_2}{\sin^2 \chi} \right), \quad (\text{II-3a})$$

$$q_2 \equiv h_2. \quad (\text{II-3b})$$

Under the gauge transformation generated by an arbitrary odd-parity vector field

$$(X_\mu) \equiv (X_\tau, X_\chi, X_\theta, X_\phi) = (0, 0, 0, C(\chi, \tau) \sin \theta \partial Y_{10}/\partial \theta), \quad (\text{II-4})$$

the functions transform as

$$\delta q_1 = 0, \quad \delta q_2 = -2C, \quad \delta h_0 = C_{,\tau} - 2R_{,\tau}C/R \quad (\text{II-5})$$

so that q_1 is gauge invariant.

The exterior line element is similarly expanded as

$$\begin{aligned} ds^2 = & -(1 - 2M/r)dt^2 + (1 - 2M/r)^{-1}dr^2 + r^2(d\theta^2 + \sin^2\theta d\phi^2) \\ & + 2\epsilon[\tilde{h}_0 \sin\theta \partial Y_{10}/\partial\theta]dt d\phi + 2\epsilon[\tilde{h}_1 \sin\theta \partial Y_{10}/\partial\theta]dr d\phi \\ & + 2\epsilon[\frac{1}{2}\tilde{h}_2(\cos\theta \partial Y_{10}/\partial\theta - \sin\theta \partial^2 Y_{10}/\partial\theta^2)]d\theta d\phi \end{aligned} \quad (\text{II-6})$$

and we define, as in equations (II-3):

$$\tilde{q}_1 \equiv \tilde{h}_1 + \frac{1}{2}r^2 \frac{\partial}{\partial r} \left(\frac{\tilde{h}_2}{r^2} \right), \quad \tilde{q}_2 \equiv \tilde{h}_2. \quad (\text{II-7})$$

Here \tilde{q}_1 is gauge invariant.

The perturbation equations for the exterior (vacuum) region are derived by Moncrief (1974) from a variational principle for the perturbation equations (wherein k_1, k_2 are written for \tilde{q}_1, \tilde{q}_2). The interior perturbation equations are given by

$$\frac{1}{R} \frac{\partial}{\partial \tau} \left\{ R^3 \frac{\partial}{\partial \tau} \left(\frac{q_1}{R^2} \right) - \frac{R^3 \sin^2 \chi}{2 \cos \chi} \frac{\partial}{\partial \chi} \left[\frac{\partial}{\partial \tau} \left(\frac{q_2}{R^2 \sin^2 \chi} \right) + \frac{2h_0}{R^2 \sin^2 \chi} \right] \right\} + \left[\frac{(l-1)(l+2)}{R^2 \sin^2 \chi} \right] q_1 = 0, \quad (\text{II-8a})$$

$$\frac{1}{2R} \frac{\partial}{\partial \tau} \left[2Rh_0 + R^3 \frac{\partial}{\partial \tau} \left(\frac{q_2}{R^2} \right) \right] - \frac{1}{R^2} \frac{\partial}{\partial \chi} [\cos \chi q_1] = 0, \quad (\text{II-8b})$$

$$\frac{1}{2} \frac{\partial}{\partial \chi} \left[\frac{\pi_1}{l(l+1)R} \right] + \frac{\cos \chi}{\sin \chi} \frac{\pi_1}{l(l+1)R} + \frac{(l-1)(l+2)}{4 \sin^2 \chi} \left[\frac{\partial}{\partial \tau} \left(\frac{q_2}{R^2} \right) + \frac{2h_0}{R^2} \right] = -8\pi\rho U, \quad (\text{II-8c})$$

in which π_1 is defined by

$$\frac{R^2 \pi_1}{l(l+1) \cos \chi} \equiv R^3 \frac{\partial}{\partial \tau} \left(\frac{q_1}{R^2} \right) - \frac{R^3 \sin^2 \chi}{2 \cos \chi} \frac{\partial}{\partial \chi} \left[\frac{\partial}{\partial \tau} \left(\frac{q_2}{R^2 \sin^2 \chi} \right) + \frac{2h_0}{R^2 \sin^2 \chi} \right] \quad (\text{II-9})$$

and U is defined in terms of the fluid velocity perturbation by

$$\partial U_\mu / \partial \epsilon|_{\epsilon=0} = [0, 0, 0, U(\chi, \tau) \sin\theta \partial Y_{10}/\partial\theta]. \quad (\text{II-10})$$

It is straightforward to verify from equations (II-5) and (II-9) that π_1 is gauge invariant and from the transformation

$$\delta U_\mu = X^\nu U_{\mu;\nu} + X^\nu_{;\mu} U_\nu \quad (\text{II-11})$$

that U is gauge invariant [$\delta U_\mu \equiv 0$ for $(U_\mu) = (-1, 0, 0, 0)$].

From equations (II-8), and the defining equation for π_1 (eq. [II-9]), one can derive

$$\partial U / \partial \tau = 0, \quad (\text{II-12a})$$

$$R^3 \frac{\partial}{\partial \tau} \left[\frac{1}{R} \frac{\partial}{\partial \tau} (R^2 \pi_1) \right] - \frac{\partial}{\partial \chi} \left[\frac{1}{\sin^2 \chi} \frac{\partial}{\partial \chi} (\sin^2 \chi R^2 \pi_1) \right] + \frac{(l-1)(l+2)}{\sin^2 \chi} R^2 \pi_1 = 16\pi\rho R^3 U_{,x} l(l+1), \quad (\text{II-12b})$$

$$\frac{1}{R} \frac{\partial}{\partial \tau} \left[R^3 \frac{\partial}{\partial \tau} \left(\frac{\cos \chi}{R^2} q_1 \right) \right] - \sin^2 \chi \frac{\partial}{\partial \chi} \left[\frac{1}{\sin^2 \chi} \frac{\partial}{\partial \chi} \left(\frac{\cos \chi}{R^2} q_1 \right) \right] + \frac{(l-1)(l+2) \cos \chi}{R^2 \sin^2 \chi} q_1 = 0. \quad (\text{II-12c})$$

Equation (II-12a) is the only nontrivial odd-parity perturbation of Euler's equations, $T_{\mu;\nu} = 0$. Equation (II-12c) is essentially the wave equation of Lifshitz and Khalatnikov (1963) which was rederived in RW formalism by Sengupta (1975). Equation (II-12b) is the basic equation we shall use since, as shown below, π_1 matches naturally to a solution of the RW wave equation in the vacuum exterior. A useful equivalent form of equation (II-12b) is:

$$\frac{\partial^2}{\partial \tau^2} (R \sin \chi \pi_1) - \frac{\partial^2}{\partial \chi^2} (R \sin \chi \pi_1) + \left[\frac{l(l+1)}{\sin^2 \chi} - \frac{3R(0)}{2R} \right] R \sin \chi \pi_1 = \frac{\sin \chi}{R} [16\pi\rho R^3 U_{,x} l(l+1)]. \quad (\text{II-13})$$

As in the work of Moncrief (1974) which used a slightly different notation, we define in the exterior region

$$\frac{\tilde{\pi}_1}{l(l+1)} = \tilde{h}_{1,t} - r^2 \frac{\partial}{\partial r} \left(\frac{\tilde{h}_0}{r^2} \right) = \tilde{q}_{1,t} - \frac{1}{2} r^2 \frac{\partial}{\partial r} \left[\frac{\tilde{q}_{2,t}}{r^2} + \frac{2\tilde{h}_0}{r^2} \right] \quad (\text{II-14})$$

and find that $r\tilde{\pi}_1$ obeys the RW equations:

$$-\frac{\partial^2}{\partial t^2} (r\tilde{\pi}_1) + \left(1 - \frac{2M}{r}\right) \frac{\partial}{\partial r} \left[\left(1 - \frac{2M}{r}\right) \frac{\partial}{\partial r} (r\tilde{\pi}_1) \right] - \left(1 - \frac{2M}{r}\right) \left[\frac{l(l+1)}{r^2} - \frac{6M}{r^3} \right] r\tilde{\pi}_1 = 0. \quad (\text{II-15})$$

It is well known that the unperturbed interior and exterior metrics match (i.e., have continuous first and second fundamental forms) across the boundary surface

$$\chi = \chi_0, \quad r = R(\tau) \sin \chi_0. \quad (\text{II-16})$$

By a suitable condition upon the gauge in a neighborhood of the boundary surface one can always require that the boundary surface of the perturbed spacetime have this same coordinate characterization. In Appendix A it is shown that the matching conditions at this boundary surface are

$$\tilde{\pi}_1 = \pi_1, \quad \tilde{n}^\mu \tilde{\pi}_{1,\mu} = n^\mu \pi_{1,\mu} + l(l+1)16\pi\rho U \quad (\text{II-17})$$

where n^μ and \tilde{n}^μ are the unit outward normal vector to the boundary surface expressed in interior and exterior coordinates, respectively.

Since $\rho R^3 = 3M/(4\pi \sin^3 \chi_0)$ and U are time independent, the source term on the right side of equation (II-12b) is time independent. We therefore seek a particular solution of the form $R^2\pi_1 = C(\chi)$ for which equation (II-12b) reduces to

$$-\frac{d}{d\chi} \left[\frac{1}{\sin^2 \chi} \frac{d}{d\chi} (\sin^2 \chi C) \right] + \frac{(l-1)(l+2)}{\sin^2 \chi} C = 16\pi\rho R^3 U_{,x} l(l+1). \quad (\text{II-18})$$

For any particular solution $C(\chi)$ of this equation we can clearly write the general solution of equation (II-12b) as

$$\pi_1 = \pi_1|_{\text{hom}} + C(\chi)/R^2, \quad (\text{II-19})$$

where $\pi_1|_{\text{hom}}$ satisfies the homogeneous equation obtained from equation (II-12b) by setting the source term to zero.

We can now derive an interesting nonradiation result analytically. Consider a source term $U(\chi)$ for which equation (II-12b) admits a solution $C(\chi)$ which is regular (as discussed in Appendix B) at $\chi = 0$ and for which the boundary values obey

$$R^2\pi_1(\chi_0, \tau) = C(\chi_0) = 0, \quad (\text{II-20a})$$

$$R^3[n^\mu \pi_{1,\mu} + 16\pi\rho U l(l+1)]|_{\chi=\chi_0} = [C_{,x} + 16\pi\rho R^3 U l(l+1)]|_{\chi=\chi_0} = 0. \quad (\text{II-20b})$$

Since C , U , and ρR^3 are all time independent, these conditions are satisfied by C at every instant if they are satisfied initially. They are thus consistent with putting $\tilde{\pi}_1 = 0$ everywhere in the exterior region and $\pi_1|_{\text{hom}} = 0$ everywhere in the interior region. That appropriate source functions $U(\chi)$ exist is obvious since we could simply choose a $C(\chi)$ satisfying the regularity and junction conditions and then define $U(\chi)$ from equation (II-18). Thus there exist non-trivial perturbations for $l \geq 2$ which are nonradiative at first order.

Now consider an arbitrary source function $U(\chi)$. We claim that one can always choose regular Cauchy data on the hypersurface of time symmetry ($\tau = t = \eta = 0$) which satisfy

$$\pi_1(0, \chi) = C(\chi)/R^2(0), \quad \partial\pi_1(0, \chi)/\partial\tau = 0, \quad \partial\tilde{\pi}_1(0, r)/\partial t = 0, \quad (\text{II-21})$$

where $C(\chi)$ is a solution of equation (II-18) and where $\tilde{\pi}_1(0, r)$ is (initially) a solution of the stationary RW equation

$$\left(1 - \frac{2M}{r}\right) \frac{\partial}{\partial r} \left[\left(1 - \frac{2M}{r}\right) \frac{\partial}{\partial r} (r\tilde{\pi}_1) \right] - \left(1 - \frac{2M}{r}\right) \left[\frac{l(l+1)}{r^2} - \frac{6M}{r^3} \right] r\tilde{\pi}_1 = 0 \quad (\text{II-22})$$

with the asymptotic form

$$r\tilde{\pi}_1 \xrightarrow{r \rightarrow \infty} q_l (2M/r)^l, \quad (\text{II-23})$$

where q_l is a constant. The choice of Cauchy data then amounts to the choice of an initially stationary exterior multipole of magnitude q_l , and an initially stationary interior solution characterized by $\pi_1|_{\text{hom}} = 0$ initially. That such a $C(\chi)$ and π_1 exist (and in fact are unique) for any regular source $U(\chi)$ is demonstrated in Appendix B, where

the explicit solution is given. The idea is simply that to any regular solution of equation (II-18) one can always add a multiple of the regular solution of the homogeneous equation. That freedom, together with the freedom to choose q_i , allows one always to satisfy the junction conditions on the initial surface. That one can also set $\pi_{1,\tau}|_{\tau=0}$ and $\tilde{\pi}_{1,t}|_{t=0} = 0$ follows from taking the τ -derivative of the junction conditions at $\tau = 0$.

The choice of $\tilde{\pi}_1$ to be initially a solution of equations (II-21), (II-22), and (II-23) is simply the natural choice of an initially stationary exterior multipole; the choice $\pi_{1|\text{hom}} = 0$ is not so easily justified. The natural candidate for the structure of the star prior to the $t = \tau = 0$ hypersurface would be the static interior Schwarzschild solution (Møller 1952), matched to the exterior Schwarzschild metric, and perturbed into slow stationary rotation. It is easy to show that this solution can be matched (continuous first and second background fundamental forms) to the Oppenheimer-Snyder solution across the $t = \tau = 0$ hypersurface.

The "lapse function" $N \equiv (-g^{00})^{-1/2}$, however, is discontinuous across this surface. An examination of the electromagnetic and scalar wave functions reveals that this discontinuity makes it impossible for the wave amplitude to have a vanishing second time derivative both prior to and subsequent to $t = \tau = 0$. Thus, our initial conditions applied to the model with a (background) Schwarzschild interior for $t \leq 0$, correspond to a perturbation which was not strictly stationary prior to the onset of collapse. If, on the other hand, we demand that the second time derivative vanish at $t = \tau = 0$, and that the wave amplitude be stationary prior to the hypersurface, then we are forced to adopt a precollapse structure which is unphysical (a star with negative uniform pressure and negative surface tension).

The real justification of setting $\pi_{1|\text{hom}} = 0$ lies in the fact that more realistic initial data do not significantly change the radiation into the exterior geometry. Preliminary work on collapses from initial radius $r_0 \geq 4M$ with a Schwarzschild interior solution as the precollapse star, indicates that a nonvanishing $\pi_{1|\text{hom}}$ field changes the radiation by no more than 1 or 2%, and has a negligible effect if the collapse starts from a nonrelativistic ($\gg M$) radius. For collapse from a large radius the reason for this is clear. The metric coefficients are determined primarily by the density distribution, which is homogeneous in both the Schwarzschild interior and in the Oppenheimer-Snyder metrics. The pressure has only a small effect. The discontinuity of the lapse function at $t = \tau = 0$ must therefore be small.

The splitting of π_1 into $\pi_{1|\text{hom}}$ and $C(\chi)$ has the following important consequence. The term $C(\chi)/R^2$ is uniquely determined by the matter distribution $U(\chi)$ and the regularity, junction, and initial conditions that we impose (see Appendix B for proof). It enters into the determination of the evolution of $\pi_{1|\text{hom}}$ and $\tilde{\pi}_1$ only through the contribution to the boundary values of π_1 and $n^\mu \pi_{1,\mu}$. Furthermore, since the time dependence of $C(\chi)/R^2$ is given *a priori*, we need only evaluate its initial surface contributions to the junction conditions in order to know these contributions for all time.

The result is particularly simple in the case $\pi_{1|\text{hom}} = 0$ initially. From the initial junction conditions (eq. [II-17]) at $R = R(0)$, $r = R(0) \sin \chi_0 \equiv r_0$, we find that

$$C(\chi_0) = R^2(0)\tilde{\pi}_1(r_0, 0), \quad (\text{II-24a})$$

$$[C_{,\chi} + 16\pi\rho R^3 U(l+1)]|_{\chi=\chi_0} = R^3(0)[\tilde{n}^\mu \tilde{\pi}_{1,\mu}]|_{r=r_0, t=0}, \quad (\text{II-24b})$$

so that the junction conditions can be rewritten as

$$\pi_{1|\text{hom}} = \tilde{\pi}_1 - \tilde{\pi}_1(r_0, 0)(r_0/r)^2, \quad (\text{II-25a})$$

$$n^\mu(\pi_{1|\text{hom}})_{,\mu} = \tilde{n}^\mu \tilde{\pi}_{1,\mu} - (r_0/r)^3[\tilde{n}^\mu \tilde{\pi}_{1,\mu}]|_{r=r_0, t=0}. \quad (\text{II-25b})$$

But the initial surface values of $\tilde{\pi}_1$ and $\tilde{n}^\mu \tilde{\pi}_{1,\mu}$ can be read directly from the initial static solution and given explicitly as functions of M , r_0 , and q_i . The wave equations for $\pi_{1|\text{hom}}$ and for $\tilde{\pi}_1$ are homogeneous, of course, and the Cauchy data for $\pi_{1|\text{hom}}$ and for $\tilde{\pi}_1$ require specifying only M , r_0 , and q_i . In consequence these three parameters suffice to specify the solution for the evolution of $\pi_{1|\text{hom}}$ and $\tilde{\pi}_1$, so that the exterior field and hence the radiation is completely determined by M , r_0 , and q_i ; no further details of the source need be given. Once $C(\chi)$ is chosen to satisfy equation (II-18) subject to boundary conditions (eq. [II-24]), the solution for $\pi_1 = \pi_{1|\text{hom}} + C(\chi)/R^2$ is also complete.

b) Electromagnetic Perturbations

One can always do "test field" electrodynamics by solving the Maxwell equations on a given spacetime background. This approach appears to ignore the possible influence of the electromagnetic fields upon the gravitational field. However, when the electromagnetic field vanishes in the background, one can regard the "test field" as a special solution of the perturbed Einstein-Maxwell system since, to first order, these equations do not couple electromagnetic and gravitational perturbations.

Let us suppose that we perturb the (neutral) Oppenheimer-Snyder collapse interior by an electromagnetic current

$$(\delta j_\mu) = (0, 0, 0, j_i(\chi, \tau) \sin \theta \partial Y_{10} / \partial \theta). \quad (\text{II-26})$$

Any such current satisfies the continuity equation $(g^{\mu\nu}\delta j_\nu)_{;\mu} = 0$ identically and drives a vector potential

$$\begin{aligned} (A_\mu) &= (0, 0, 0, a(\chi, \tau) \sin \theta \partial Y_{10}/\partial \theta) \quad (\text{interior}), \\ (\tilde{A}_\mu) &= (0, 0, 0, \tilde{a}(r, t) \sin \theta \partial Y_{10}/\partial \theta) \quad (\text{exterior}). \end{aligned} \quad (\text{II-27})$$

The equation of motion for \tilde{a} was first derived by Regge and Wheeler (1957). The interior equation for a is given by

$$\frac{1}{R} \frac{\partial}{\partial \tau} \left(R \frac{\partial a}{\partial \tau} \right) - \frac{1}{R^2} \frac{\partial^2 a}{\partial \chi^2} + \frac{l(l+1)}{R^2 \sin^2 \chi} a = 4\pi j_l, \quad (\text{II-28})$$

while the exterior (RW) equation is

$$\frac{\partial^2 \tilde{a}}{\partial t^2} - \left(1 - \frac{2M}{r}\right) \frac{\partial}{\partial r} \left[\left(1 - \frac{2M}{r}\right) \frac{\partial \tilde{a}}{\partial r} \right] + \left(1 - \frac{2M}{r}\right) \frac{l(l+1)}{r^2} \tilde{a} = 0. \quad (\text{II-29})$$

The standard junction conditions imply the following equalities at the stellar boundary:

$$a = \tilde{a}, \quad n^\mu a_{;\mu} = \tilde{n}^\mu \tilde{a}_{;\mu}. \quad (\text{II-30})$$

In the gravitational case, the evolution of the source field was determined by the Euler equations; here it must be specified. The interior equation will admit a time-independent solution only if

$$\partial(R^2 j_l)/\partial \tau = 0, \quad (\text{II-31})$$

in which case a may be separated into a homogeneous part and a time-independent particular part, as was possible for the gravitational perturbations. This is the natural choice if we consider the collapsing star to be highly conducting. In the absence of radiation from the exterior we would then demand that in the rest frame of the fluid no electric field develop, or, from equation (II-27),

$$F_{0\phi} = a_{;\tau} \sin \theta \partial Y_{10}/\partial \theta = 0, \quad (\text{II-32})$$

which requires $a_{;\tau} = 0$.

Equivalently we can show that $a_{;\tau} = 0$ implies flux conservation. Let $\Sigma(0)$ be an arbitrary oriented two dimensional surface lying within the $\tau = 0$ hypersurface of the collapsing fluid and bounded by a curve $\partial\Sigma(0)$. We can extend $\Sigma(0)$ and its boundary $\partial\Sigma(0)$ to a one-parameter family of surfaces and boundary curves $\Sigma(\tau)$, $\partial\Sigma(\tau)$ by letting each point comove with the (unperturbed) fluid. By construction $\Sigma(\tau_0)$ and $\partial\Sigma(\tau_0)$ lie in the hypersurface $\tau = \tau_0$. For any solution of the Maxwell equations we can define the magnetic flux \mathcal{F} through $\Sigma(\tau)$ by

$$\mathcal{F}[\Sigma(\tau)] = \int_{\Sigma(\tau)} F_{\mu\nu} dx^\mu \wedge dx^\nu, \quad (\text{II-33a})$$

where

$$\frac{1}{2} F_{\mu\nu} dx^\mu \wedge dx^\nu = d[A_\mu dx^\mu], \quad (\text{II-33b})$$

$$F_{\mu\nu} = A_{\nu,\mu} - A_{\mu,\nu}. \quad (\text{II-33c})$$

It is now straightforward to show that $a_{;\tau} = 0$ is equivalent to flux conservation

$$\partial\mathcal{F}[\Sigma(\tau)]/\partial\tau = 0, \quad (\text{II-34})$$

i.e., to the magnetic field being "frozen into" the collapsing fluid.

By equation (II-28) we see that $a_{;\tau} = 0$ requires $j_l R^2$ to be independent of τ , and we take this as our evolution law. Even with this condition, of course, we do not expect $a(\chi, \tau)$ to remain time independent since the collapse will produce (except in special cases) a radiation field $a|_{\text{hom}}$ which can contribute a time-dependent flux through $\Sigma(\tau)$.

With condition (II-31) imposed on $j_l(\chi, \tau)$, the interior equation admits a static solution, and we can write in analogy with equation (II-19)

$$a = a|_{\text{hom}} + C(\chi), \quad (\text{II-35})$$

where $C(\chi)$ satisfies the static form of equation (II-28):

$$-\frac{\partial^2 C}{\partial \chi^2} + \frac{l(l+1)}{\sin^2 \chi} C = 4\pi R^2 j_l. \quad (\text{II-36})$$

We choose Cauchy data on the initial hypersurface ($t = \eta = \tau = 0$) similar to the choice for the gravitational problem. The initial exterior function $\tilde{a}(0, r)$ is chosen to be a static solution of equation (II-29) such that

$$\tilde{a}(0, r) \xrightarrow{r \rightarrow \infty} q_i(2M/r)^l, \quad \partial \tilde{a}(0, r)/\partial t = 0, \quad (\text{II-37})$$

representing an initially static multipole. The initial interior solution is chosen such that

$$\partial a(0, \chi)/\partial \tau = 0, \quad a(0, \chi) = C(\chi); \quad (\text{II-38})$$

that is, as in the gravitational case, we choose $a|_{\text{hom}} = 0$ initially. The proof that this can be done is essentially similar to that given for the gravitational case in Appendix B.

The values of $C(\chi_0)$ and $C_{,\chi}|_{\chi_0}$ are fixed by the initial junction conditions. When these values are put into the junction conditions (eq. [II-30]), they become

$$\begin{aligned} a|_{\text{hom}} &= \tilde{a} - \tilde{a}(0, r_0), \\ n^\mu(a|_{\text{hom}})_{,\mu} &= \tilde{n}^\mu \tilde{a}_{,\mu} - (r_0/r)[\tilde{n}^\mu \tilde{a}_{,\mu}]_{t=0}. \end{aligned} \quad (\text{II-39})$$

Since the initial surface values of a and $\tilde{n}^\mu \tilde{a}_{,\mu}$ are determined by q_i , M , r_0 , we have, in complete analogy with the gravitational case, that specification of these three numbers completely fixes the evolution of $a|_{\text{hom}}$ and \tilde{a} . No additional details of the source need be given.

III. NUMERICAL RESULTS

a) Wave Equations in Characteristic Coordinates

The equations developed in the previous section are to be used to find the field that develops when an initially stationary star, with an initially stationary multipole field, collapses. The problem is pictured in Figure 1, in characteristic coordinates, so that ingoing and outgoing null lines are at 45° in this representation. The mathematical problem consists of solving an inhomogeneous wave equation in the stellar interior, and a homogeneous wave equation in the exterior, subject to boundary conditions relating the two wave functions at the stellar surface.

In the exterior the characteristic coordinates are taken to be retarded and advanced time:

$$\tilde{u} \equiv t - r_*, \quad \tilde{v} \equiv t + r_*. \quad (\text{III-1})$$

For both the gravitational and the electromagnetic case the exterior wave equation (cf. eqs. [II-15], [II-29]) may be written

$$4\partial^2 \tilde{\psi} / \partial \tilde{u} \partial \tilde{v} + \tilde{V} \tilde{\psi} = 0, \quad (\text{III-2a})$$

where

$$\tilde{\psi}_A \equiv \tilde{a}(t, r), \quad \tilde{\psi}_G \equiv r \tilde{\pi}_1(t, r), \quad (\text{III-2b})$$

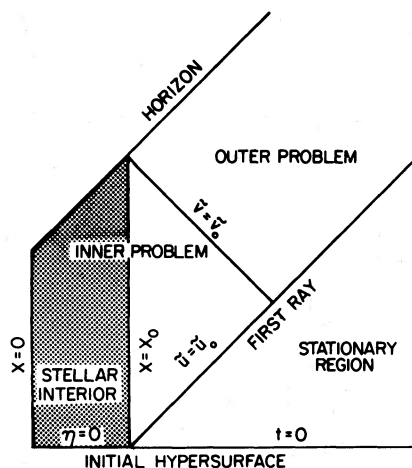


FIG. 1.—Regions of the collapse spacetime for constant θ and ϕ , pictured in characteristic coordinates. The initial perturbation field is stationary on the initial hypersurface and remains stationary (in the “stationary region”) until information on the first ray signals the onset of collapse. The inner problem is numerically solved using characteristic coordinates equal to $\eta \pm \chi$ in the Oppenheimer-Snyder interior and extended outward smoothly across the stellar surface. The outer problem is solved numerically with characteristic coordinates $t \pm r_*$. See text for further details.

and where the curvature potentials are

$$\tilde{V}_A \equiv (1 - 2M/r)l(l+1)/r^2, \quad (\text{III-3a})$$

$$\tilde{V}_G \equiv (1 - 2M/r)[l(l+1) - 6M/r]/r^2. \quad (\text{III-3b})$$

We use here subscripts A and G to denote electromagnetic and gravitational quantities, respectively; as in the previous section, a tilde ($\tilde{}$) is used to distinguish quantities in the exterior from those in the interior.

Part of the Cauchy data is based on the requirement that the exterior field consist of an initially stationary multipole, so that, at $t = 0$, $\partial\tilde{\psi}/\partial t = 0$, and $\tilde{\psi}(r_*, t = 0)$ is a solution of

$$\partial^2\tilde{\psi}/\partial r_*^2 = \tilde{V}\tilde{\psi}, \quad (\text{III-4})$$

which is well behaved at $r_* = \infty$. When we require (eqs. [II-23], [II-37]) that

$$\tilde{\psi}(r_*, 0) \xrightarrow{r_* \rightarrow \infty} q_l(2M/r)^l, \quad (\text{III-5})$$

the unique solution can be written as

$$\begin{aligned} \tilde{\psi}(r_*, 0) &= q_l(2M/r)^l F(a, b; c; [2M/r]), \\ a_A &= l, \quad a_G = l - 1, \quad b_A = l + 2, \quad b_G = l + 3, \quad c_A = c_G = 2l + 2, \end{aligned} \quad (\text{III-6})$$

where F is the hypergeometric function.

Since the Cauchy data in the exterior are stationary, the solution will remain stationary in the exterior at any point which has not yet received information from the collapsing interior. The outgoing null line labeled "first ray" in Figure 1 separates the stationary region from the dynamic region at later retarded time. In the numerical solution of the partial differential system, we use the stationary solution as characteristic data on this first ray, rather than as Cauchy data on the exterior initial hypersurface.

For the interior we can achieve significant simplification by choosing as our field variables

$$\psi_A = a|_{\text{hom}} = a - C_A(\chi), \quad \psi_G = R \sin \chi \pi_1|_{\text{hom}} = \sin \chi (R\pi_1 - C_G(\chi)/R), \quad (\text{III-7})$$

in which the functions $C(\chi)$ are the functions, discussed in the previous section, which satisfy the interior wave equation and, on the initial hypersurface, the matching conditions. In terms of the ψ variables of equation (III-7) the interior wave equations (II-12b), (II-28) are homogeneous equations of the form

$$4\partial^2\psi/\partial u\partial v + V\psi = 0. \quad (\text{III-8})$$

Here u and v are characteristic coordinates in the interior

$$u \equiv \eta - \chi, \quad v \equiv \eta + \chi, \quad (\text{III-9})$$

and the potentials are

$$V_A = l(l+1)/\sin^2 \chi, \quad (\text{III-10a})$$

$$V_G = l(l+1)/\sin^2 \chi - (3/2)R(0)/R(\eta). \quad (\text{III-10b})$$

When definitions (III-7) are substituted in the junction conditions (eqs. [II-25], [II-39]) we get

$$\begin{aligned} \psi_A &= \tilde{\psi}_A - [\tilde{\psi}_A]_{\text{in}}, \quad n^\mu \psi_{A,\mu} = \tilde{n}^\mu \tilde{\psi}_{A,\mu} - (r_0/r)(1 - 2M/r_0)^{1/2} [\tilde{\psi}_{A,r}]_{\text{in}}, \\ \psi_G &= \tilde{\psi}_G - (r_0/r)[\tilde{\psi}_G]_{\text{in}}, \quad n^\mu \psi_{G,\mu} = \tilde{n}^\mu \tilde{\psi}_{G,\mu} - (r_0/r)^2(1 - 2M/r_0)^{1/2} [\tilde{\psi}_{G,r}]_{\text{in}}. \end{aligned} \quad (\text{III-11})$$

Here the subscript "in" denotes evaluation at $t = \eta = \tau = 0$, and it is understood that equations (III-11) are to be evaluated at the stellar surface.

b) The Inner Problem

The problem is now completely specified in either the electromagnetic or gravitational case by (i) wave equations in characteristic form (III-2) and (III-8), (ii) junction equation (III-11), (iii) characteristic data (eqs. [III-6]) on the first ray, (iv) Cauchy data $\psi = 0$ and $\partial\psi/\partial\eta = 0$ at $\eta = 0$ in the interior. To solve the problem numerically, it is convenient to split the dynamical region of the spacetime in Figure 1 into two regions separated by the ingoing characteristic $v = \tilde{v}_0$ which intersects the star's surface at the event horizon. The exterior region for which $\tilde{v} < \tilde{v}_0$ may be covered with an extension of the inner characteristic coordinates by relabeling the rays $\tilde{u} = \text{const.}$, $\tilde{v} = \text{const.}$, with the u and v values, respectively, that they assume at the star's surface. This extension of coordinates is well behaved everywhere. In these coordinates the junction conditions become particularly simple since $n = R^{-1}(\partial/\partial v - \partial/\partial u)$.

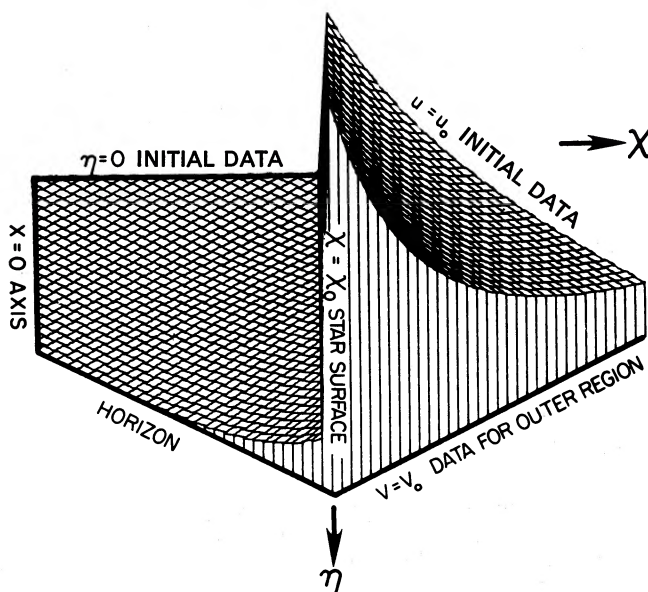


FIG. 2.—The wave functions ψ_G and $\bar{\psi}_G$ for an $l = 2$ gravitational perturbation, for the collapse from $r_0 = 4M$. The height of the surface above the base plane represents the magnitude of the wave function. The discontinuity in the figure is equal to the particular part of the interior solution, which is not included in ψ_G . See text for further details.

The numerical solution for ψ_G and $\bar{\psi}_G$ for this “inner problem” is shown in Figure 2 for the case of gravitational quadrupole perturbations of collapse from an initial radius $r_0 = 4M$. (It should be noted that the discontinuity evident in the figure arises because ψ_G represents only the homogeneous part of the field; the total field is, of course, continuous across the stellar surface.) Two points are of particular interest: First, the interior homogeneous field does not depart significantly from $\psi_G = 0$. In fact, in all cases studied the interior homogeneous field never exceeds 20% of the total field at the star’s surface, during the collapse from $r = r_0$ to $r = 2M$, so that the dynamics of the field in the interior of the star plays an unimportant role in determining the exterior radiation. We shall explore this theme in a later paper. If we ignore the homogeneous interior fields, a good approximation for the values of the field ($\bar{\psi}$)_s at the stellar surface follows from equation (III-11):

$$(\bar{\psi}_A)_s \approx [\bar{\psi}_A]_{\text{ln}} = C_A(\chi_0), \quad (\bar{\psi}_G)_s \approx (r_0/r)[\bar{\psi}_G]_{\text{ln}} = \sin^2 \chi_0 C_G(\chi_0)/r. \quad (\text{III-12})$$

Second, neither the interior nor the exterior field develops ripples that explain the oscillatory radiation found outside ($\bar{v} > \bar{v}_0$) this region.

c) The Outer Problem

The solution of the “inner problem” on $\bar{v} = \bar{v}_0$ gives us characteristic data for the solution of the “outer problem,” the determination of the field in the dynamical region for which $\bar{v} \geq \bar{v}_0$. The stationary exterior solution on the “first ray” $\bar{u} = \bar{u}_0$ completes the specification of the exterior problem. In Figure 3 numerical results are shown for $\bar{\psi}_G$, in the exterior region, for the same collapses as pictured in Figure 2. We note in this figure the emergence of a wavelike oscillation which is outgoing at large r_* and ingoing near the horizon. Figure 4 shows the location of the peak of this wave in t, r_* coordinates and compares it with the quadrupole curvature potential V_G . The interpretation suggested by this picture is clearly that the wave originates in the region of spacetime in which the potential is strong.

Numerical results are given in Figure 5 for the exterior fields from collapses starting from $r_0 = 4M$ and $r_0 = 8M$. The values of $\bar{\psi}_A$ and $\bar{\psi}_G$ at $r \approx 40M$ are normalized to unity at their peaks and plotted as functions of time. In all the plots the curves for collapse from $r_0 = 4M$ have been shifted to align the late time nodes with those for collapse from $r_0 = 8M$. The field starts from its stationary value and (at least in the case of $r_0 = 8M$) undergoes a relatively long initial dynamical phase. For collapse from larger r_0 this initial phase would be yet longer.

The striking feature of Figures 5 is not this initial phase but the damped sinusoidal oscillations in which the fields attain their peak value and in which most of the energy is radiated. The frequency and damping rate of this ringing is independent of the initial radius of the collapse and, in fact, of all details of the collapse. This is precisely the behavior expected of fields exhibiting the quasinormal modes of the black hole and will be discussed in some detail in § IVb.

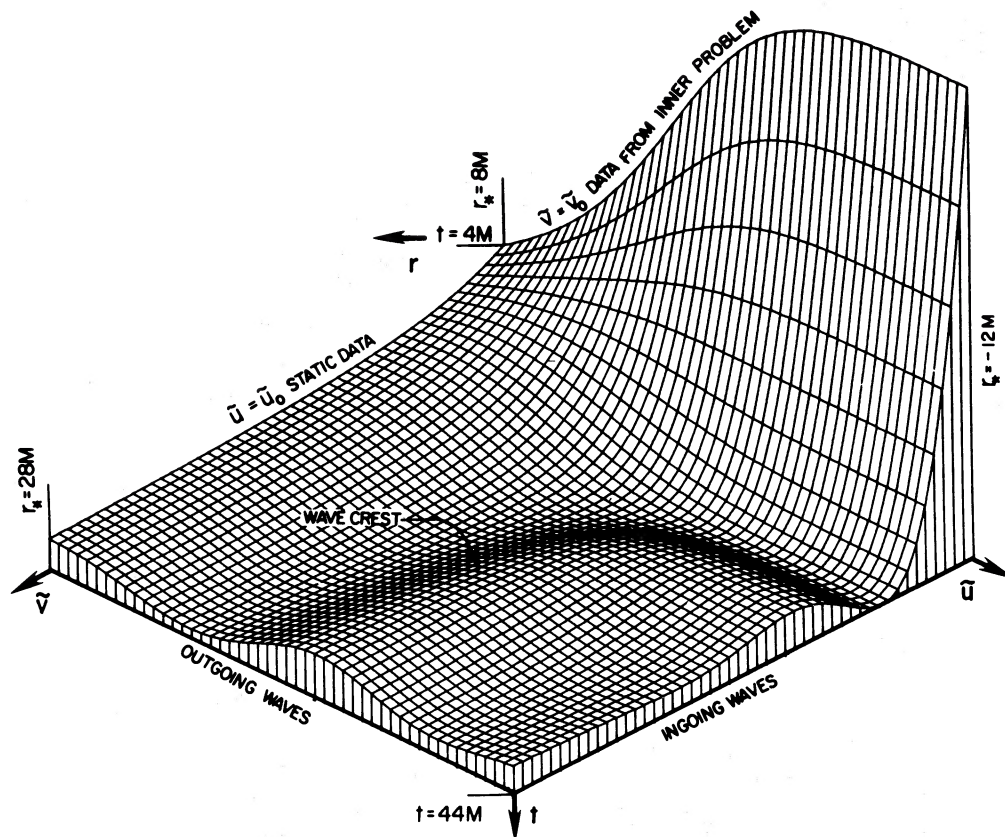


FIG. 3.—The wave function \tilde{u}_0 in the outer region for the collapse shown in Fig. 2. Waves develop in this region even though there are none in the inner problem, and the data on the outgoing first ray $u_0 = \tilde{u}_0$ is stationary. A wave crest of this radiation is indicated.

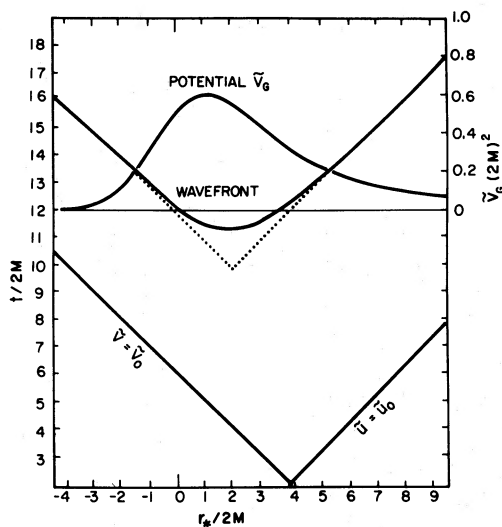


FIG. 4.—The location, in r_* , t coordinates, of the wave crest indicated in Fig. 3. The potential \tilde{V}_0 for $l = 2$ is also shown as a function of radius. The figure suggests that the wave is generated in the region of spacetime where the potential is large.

d) *Modified Collapses*

It may be asked whether the picture of an initial phase followed by ringing is in any way an idiosyncrasy of free-fall (i.e., Oppenheimer-Snyder) collapse. To investigate this, we consider a new spacetime for the stellar interior:

$$ds^2 = a^2(\eta)[-d\eta^2 + d\chi^2 + \sin^2 \chi(d\theta^2 + \sin^2 \theta d\phi^2)], \quad (\text{III-13a})$$

$$a(\eta) = \frac{1}{2}a_0(1 + \cos[\eta/\bar{\eta}]), \quad (\text{III-13b})$$

matched to a Schwarzschild exterior with mass M and initial radius satisfying

$$M = \frac{1}{2}a_0 \sin^3 \chi_0,$$

$$r(\tau) = a(\tau) \sin \chi_0,$$

$$\tau = \frac{1}{2}a_0[\eta + \bar{\eta} \sin(\eta/\bar{\eta})]. \quad (\text{III-14})$$

For the choice $\bar{\eta} = 1$ this is the usual Oppenheimer-Snyder collapse, but a choice of $\bar{\eta} > 1$ gives a slower collapse. Since the second fundamental form is not continuous across the stellar collapse for $\bar{\eta} \neq 1$, the collapsing star is rather unusual: a homogeneous star with uniform negative pressure surrounded by a shell containing time-dependent mass and negative surface tension. The collapse is slowed as if the interior were hung from the somewhat rigid (negative surface tension) shell, and we shall call such stars "drumhead" models.

Drumhead stars of course cannot be taken at all seriously as stellar models. They do, however, provide analytic non-free-fall collapses for which all the equations and numerical techniques of this section apply, at least for electromagnetic perturbations. (In a subsequent paper the collapse of more realistic stellar models will be investigated.) The wave function for electromagnetic dipole radiation is shown in Figure 6 for $\bar{\eta} = 1$ (Oppenheimer-Snyder), $\bar{\eta} = 2$, and $\bar{\eta} = 3$, with the curves shifted so that late time nodes align. It is clear that the effect of $\bar{\eta} \neq 1$ is not only to lengthen the initial phase (slow down the collapse) but also to decrease the strength of excitation of the ringing. The ringing is still characterized in all cases by a single frequency and a single damping rate, and the ringing still accounts for most of the oscillation in the wave functions.

e) *Spectra and Total Energy*

To relate the wave functions to observed power flux and spectra, we first note that in the electromagnetic case the vector potential of equation (II-27) implies that far from the star the electric vector is

$$\mathbf{E} = \frac{1}{r} \left(\frac{\partial}{\partial \bar{u}} \bar{\psi}_A \right) \left(\frac{\partial}{\partial \theta} Y_{10} \right) \mathbf{e}_{[\phi]}, \quad (\text{III-15})$$

where $\mathbf{e}_{[\phi]}$ is the physical (unit) basis vector in the ϕ direction. The power radiated per unit solid angle is then given by the Poynting vector in the radiation zone

$$\frac{d \text{Power}}{d\Omega} = \frac{r^2}{4\pi} |\mathbf{E}|^2 = \frac{1}{4\pi} \left| \frac{\partial}{\partial \bar{u}} \bar{\psi}_A \right|^2 \left| \frac{\partial}{\partial \theta} Y_{10} \right|^2, \quad (\text{III-16})$$

and the total power is

$$\text{Power} = \frac{1}{4\pi} \frac{(l+1)!}{(l-1)!} \left| \frac{\partial}{\partial \bar{u}} \bar{\psi}_A \right|^2. \quad (\text{III-17})$$

For gravitational radiation the analogs of the electric and magnetic fields are the metric perturbations $h_{\theta\theta}$, $h_{\phi\phi}$, $h_{\theta\phi}$ in the radiation gauge, the gauge in which the physical components $h_{[\theta][\theta]}$, $h_{[\theta][\phi]}$, $h_{[\phi][\phi]}$ fall off as r^{-1} \times functions of $(t - r_*)$, and in which all other physical components fall off as $1/r^2$ or faster. In this gauge the radiated power (Landau and Lifshitz 1975) is

$$\frac{d \text{Power}}{d\Omega} = \frac{1}{16\pi} r^2 \left[\left(\frac{\partial}{\partial \bar{u}} h_{[\theta][\phi]} \right)^2 + \frac{1}{4} \left(\frac{\partial}{\partial \bar{u}} h_{[\theta][\theta]} - \frac{\partial}{\partial \bar{u}} h_{[\phi][\phi]} \right)^2 \right], \quad (\text{III-18})$$

and for an axisymmetric odd-parity perturbation $h_{[\theta][\theta]} = h_{[\phi][\phi]} = 0$. From the definitions of the h 's (eq. [II-6]) we have that

$$h_{[\theta][\phi]} = (1 - 2M/r)^{-1/2} \tilde{h}_0 \frac{\partial Y_{10}}{\partial \theta} \quad (\text{III-19a})$$

$$h_{[\theta][\theta]} = \frac{1}{2} r^{-2} \tilde{h}_2 \left(\cot \theta \frac{\partial Y_{10}}{\partial \theta} - \frac{\partial^2 Y_{10}}{\partial \theta^2} \right), \quad (\text{III-19b})$$

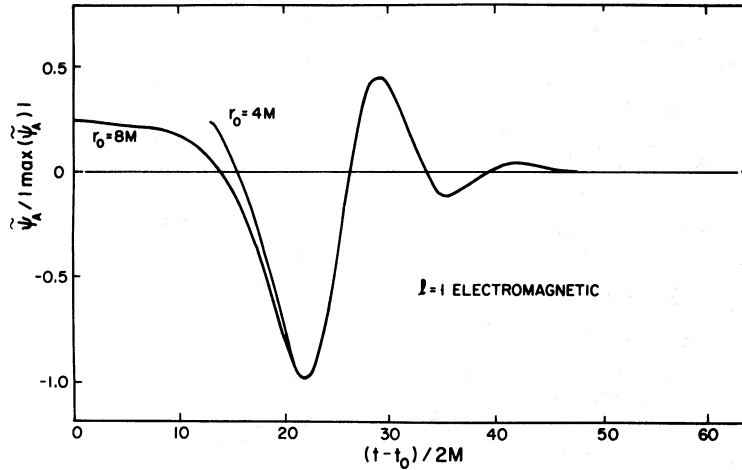


FIG. 5a

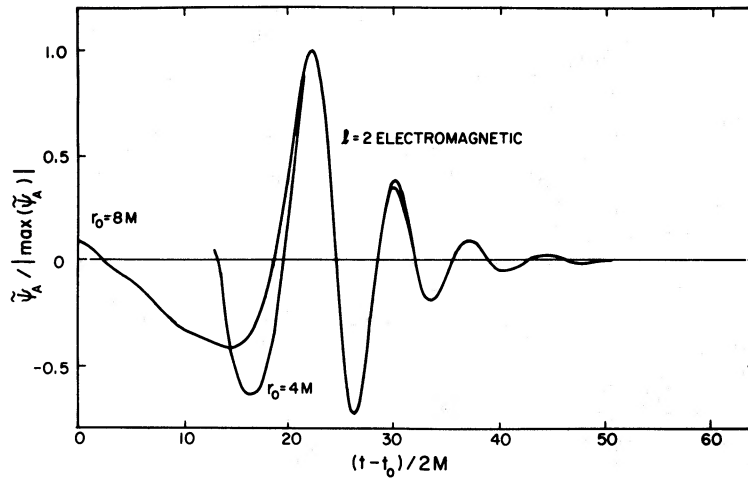


FIG. 5b

FIG. 5.—(a)–(d) The exterior wave functions ψ_A and ψ_G at $r \approx 40 M$ as a function of time $t - t_0$ after passage of the first ray, for several multipoles, for collapse from $r_0 = 4M$ and $8M$. The curves are normalized to a maximum of unity at their peaks, and the $r_0 = 4M$ curves are shifted so that late time nodes are aligned with those for $r_0 = 8M$.

and from the equations in the exterior (Moncrief 1974) we also have

$$\frac{\partial}{\partial \bar{u}} \tilde{h}_2 = -2 \frac{(l-2)!}{(l+2)!} (1 - 2M/r)(\tilde{\psi}_G + r\tilde{\psi}_{G,r}) - 2\tilde{h}_0. \tag{III-20}$$

In the radiation gauge, equation (III-19a) implies that $\tilde{h}_0 = \mathcal{O}(1/r)$ and equations (III-19b) and (III-20) require that $\tilde{\psi}_G = \mathcal{O}(1)$ so that

$$\tilde{\psi}_{G,r} = (1 - 2M/r)^{-1} \tilde{\psi}_{G,r} = -(1 - 2M/r)^{-1} \frac{\partial}{\partial \bar{u}} \tilde{\psi}_G + \mathcal{O}(1/r). \tag{III-21}$$

The power flux is therefore

$$\frac{d \text{Power}}{d\Omega} = \frac{1}{16\pi} \left[\frac{(l-2)!}{(l+2)!} \right]^2 \left[\frac{\partial}{\partial \bar{u}} \tilde{\psi}_G \right]^2 \left(\cot \theta \frac{\partial Y_{l0}}{\partial \theta} - \frac{\partial^2 Y_{l0}}{\partial \theta^2} \right)^2, \tag{III-22}$$

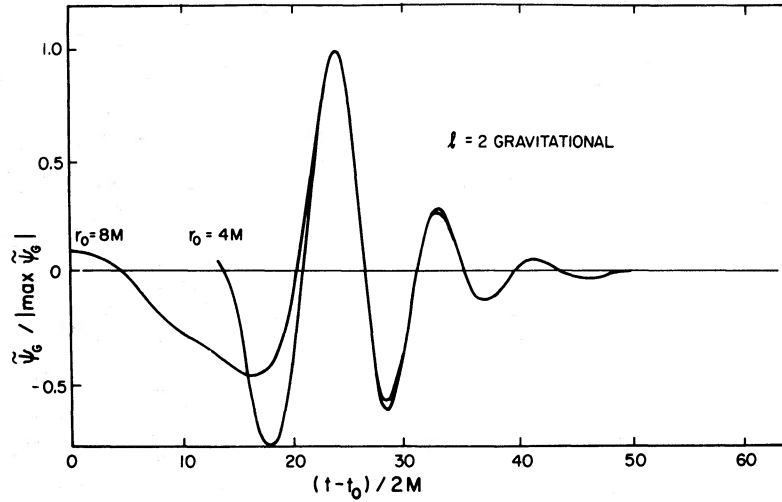


FIG. 5c

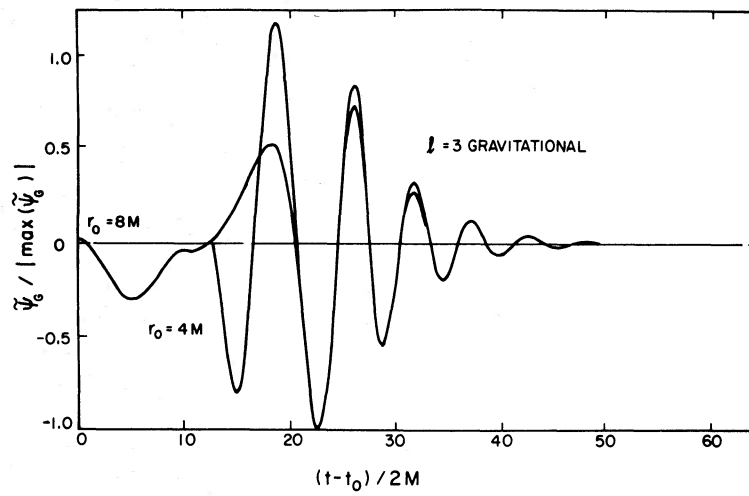


FIG. 5d

FIG. 5.—Continued

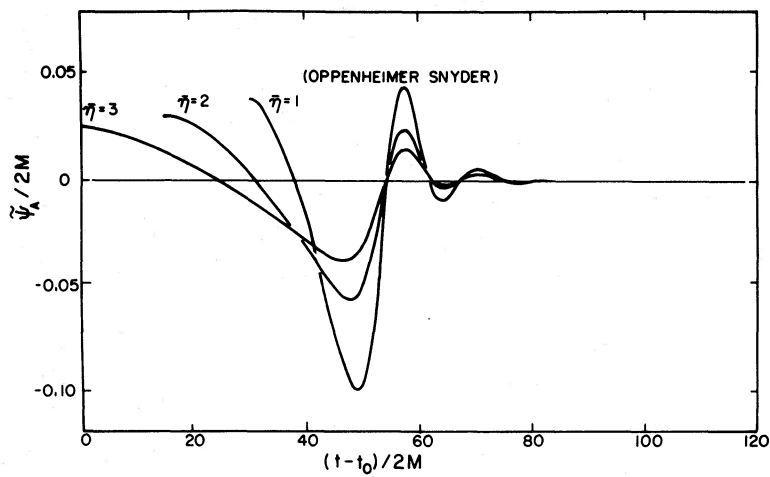


FIG. 6.—Dipole electromagnetic radiation for modified (“drumhead”) collapses. The interior dynamics of the background collapse is similar to the Oppenheimer-Snyder collapse, but the expansion factor is taken to be $a(\eta) = (a_0/2)(1 + \cos[\eta/\bar{\eta}])$. (See text for details.) Curves are shown for $\bar{\eta} = 2, 3$ as well as for the Oppenheimer-Snyder case $\bar{\eta} = 1$. All collapses start from $r_0 = 8M$.

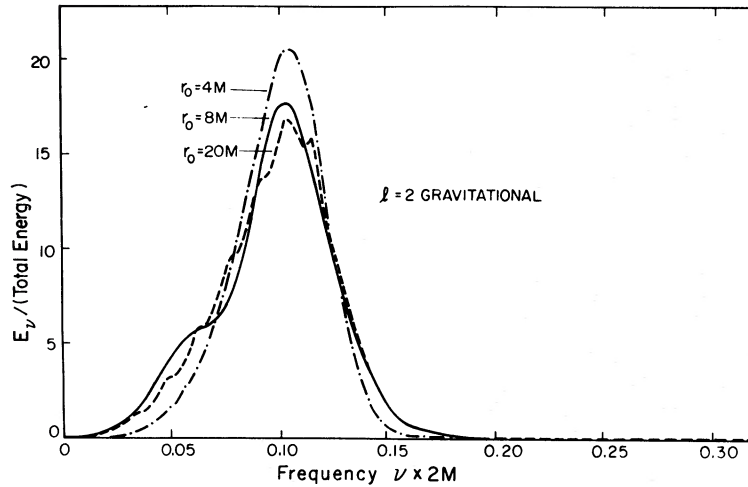


FIG. 7.—The spectra of gravitational quadrupole radiation reaching a distant observer for collapses from three different initial radii. Plotted is the ratio E_ν/E of energy per unit frequency to total energy, as a function of frequency ν . The strong similarity of these spectra suggests that ringing radiation, the spectrum of which is independent of details of the collapse, carries most of the energy radiated.

which, when integrated over solid angle, gives the total power

$$\text{Power} = \frac{1}{16\pi} \frac{(l-2)!}{(l+2)!} \left[\frac{\partial}{\partial \bar{u}} \bar{\psi}_G \right]^2. \quad (\text{III-23})$$

For both the electromagnetic and gravitational wave functions we define the Fourier transforms

$$g(\omega) = \int_{-\infty}^{+\infty} \left(\frac{\partial}{\partial \bar{u}} \bar{\psi} \right) e^{-i\omega \bar{u}} d\bar{u} \quad (\text{III-24})$$

so that the energy per unit frequency is

$$\begin{aligned} E_\nu &\equiv d \text{Energy} / d\nu = 2\kappa |g|^2, \\ \kappa_A &= (4\pi)^{-1} [(l+1)! / (l-1)!], \\ \kappa_G &= (16\pi)^{-1} [(l-2)! / (l+2)!], \\ \nu &\equiv \omega / 2\pi. \end{aligned} \quad (\text{III-25})$$

Figure 7 shows the spectra for gravitational quadrupole radiation for collapses from three initial radii. Plotted is the quantity $E_\nu/(\text{total energy})$ so the curves all enclose unit area. The radiation emitted in these collapses has a sharply defined frequency: the spectra are quite narrow, an indication of the importance of ringing radiation in this problem. Figure 5*b* shows that it is the behavior of the wave function immediately after the collapse, rather than at late times, which is influenced by the initial radius of the collapse. Therefore, it is these differences in this early-time behavior which produce the differences among the three spectra. The initial radiation emitted by a collapse from a large radius has, typically, a lower frequency than the ringing radiation which will follow, and the spectra differ primarily at low frequencies. However, the early radiation seems to boost the peak of the spectrum for the collapse from $r_0 = 4M$.

Figure 8 shows normalized spectra for radiation in several different modes for collapses from $r_0 = 4M$. The spectra are all fairly narrow band in character and similar to those in Figure 7. We shall see in § IV*b* that the narrow band character can be understood in terms of ringing at the quasi-normal frequencies. (The small secondary peaks in the octupole spectra are caused by early-time behavior and do not indicate a higher frequency quasi-normal ringing.) The total energy radiated for $l = 1, 2, 3$ is plotted as a function of initial radius r_0 in Figure 9 for both the electromagnetic and the gravitational case.

IV. DISCUSSION

a) Power-Law Tails

Figures 5 suggest that after an initial burst of radiation the fields fall off as damped sinusoids, but in fact at very late times this is not true. Figures 10, logarithmic plots of the time dependence of the fields at late times, show that

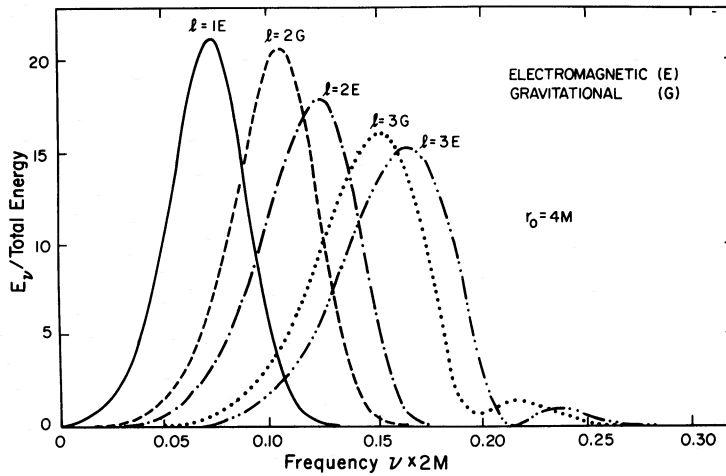


FIG. 8.—The spectra of radiation emitted in several different modes from an $r_0 = 4M$ collapse. Note that in all cases the energy radiated is significant only over a narrow frequency band.

in fact at very late times the fields develop power-law tails.¹ The nature of these tails of the radiation in a Schwarzschild background has been analyzed in some detail by Price (1972), and we summarize here the relevant results:

Long after the collapse, in the region of spacetime for which $|t/r_*| \gg 1$ an initially stationary multipole perturbation will have the form

$$\tilde{\psi} = (2M/t)^{2l+2\bar{\eta}}\Psi(r)[1 + \mathcal{O}(t^{-1})]. \tag{IV-1}$$

¹ The tails are nonradiative, carry no power, and are unimportant in an astrophysical context.

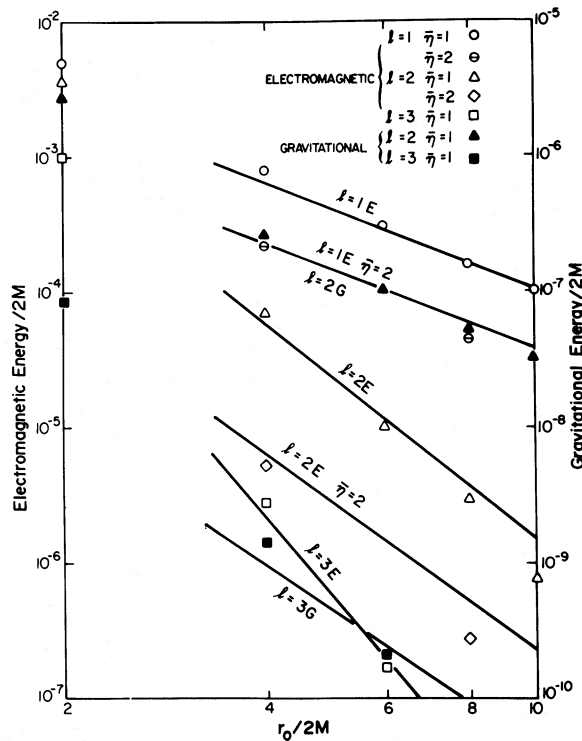
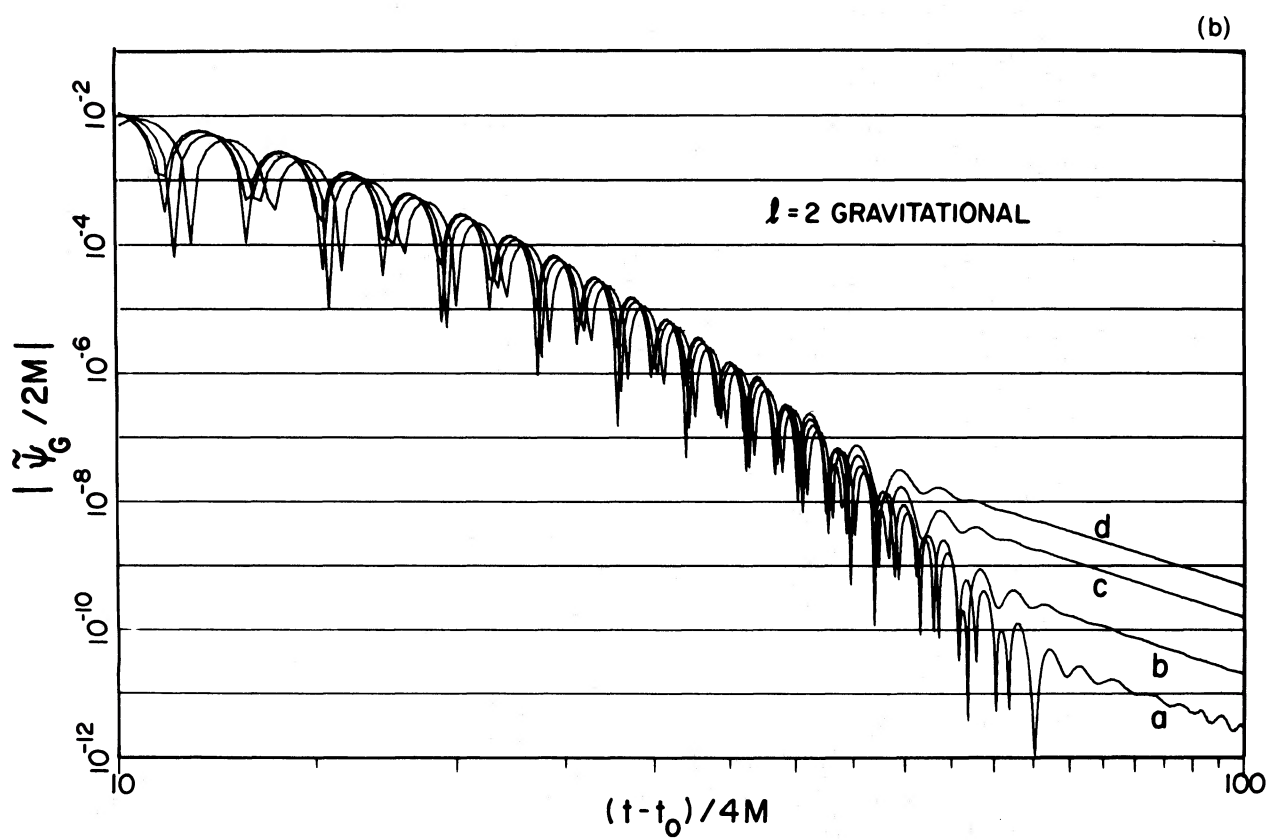
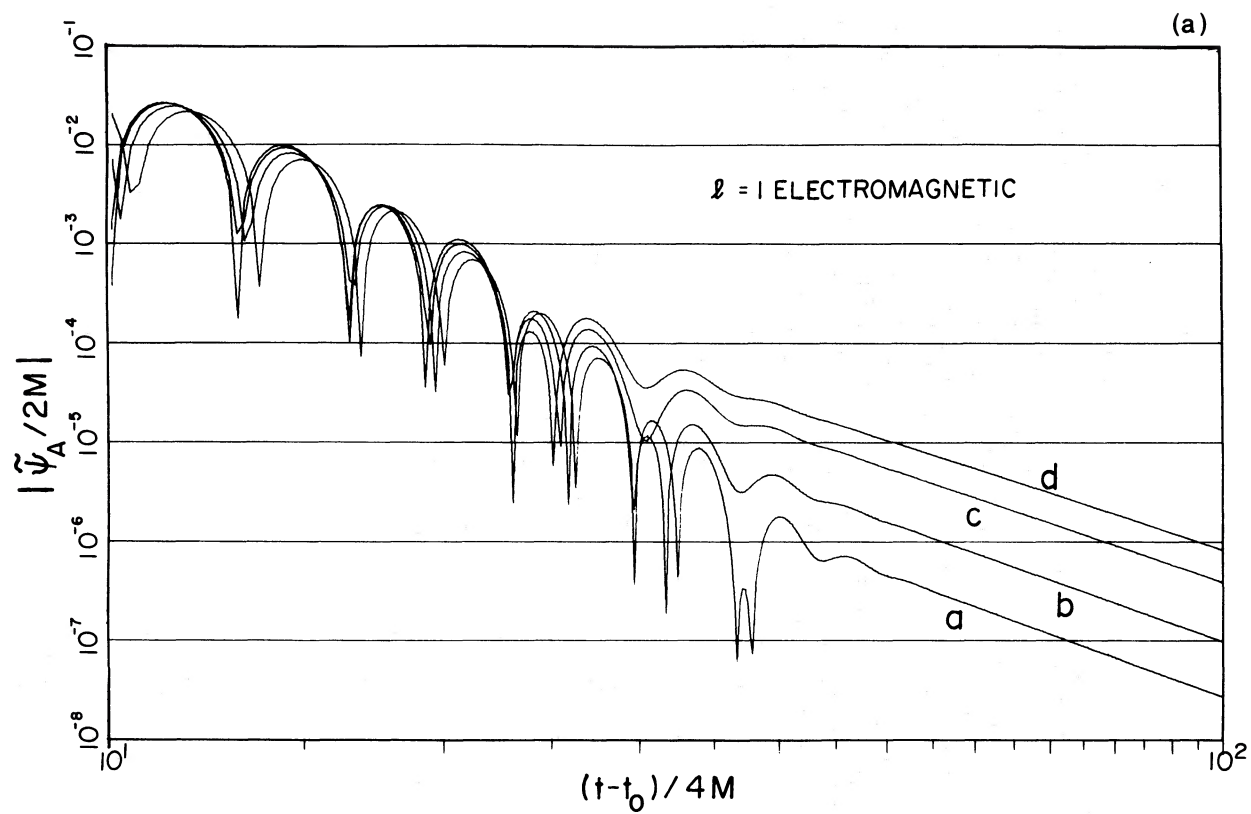


FIG. 9.—The total energy radiated in different modes as a function of initial radius r_0 of collapse. Initial multipole moments $q_l/2M$ are taken to be unity. Points on the graph indicate the results of numerical computations for electromagnetic and gravitational radiation for Oppenheimer-Snyder ($\bar{\eta} = 1$) collapses as well as for “drumhead” ($\bar{\eta} = 2, 3$) models. The curves represent an approximation based on the assumption that the energy is mostly due to quasi-normal ringing. (See § IVb of text for details.)



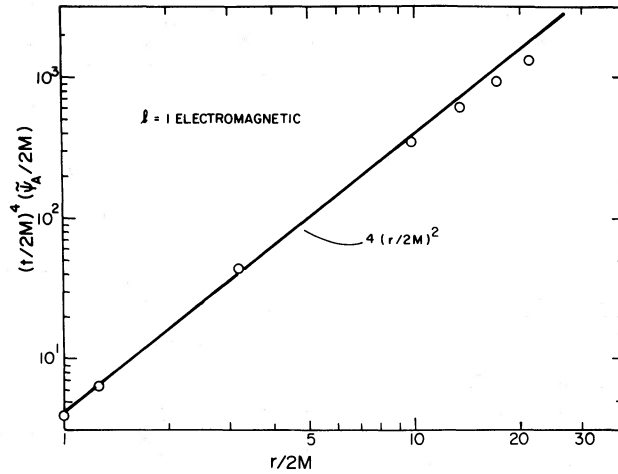


FIG. 11.—Radial dependence of the dipole electromagnetic late-time tail for collapse from $r_0 = 4M$, with an initial unit dipole moment ($q_i/2M = 1$). The solid line represents the predicted behavior $(\tilde{\Psi}_A/2M) \rightarrow 4(2M/t)^4(r/2M)^2$. The points are the numerical results from the solution of the wave equations.

Here Ψ is a stationary solution of the wave equation (cf. eq. [III-6]) with the following properties: (i) At large r (that is, $r/2M \gg 1$), Ψ becomes

$$\Psi = q_i C_l (r/2M)^{l+1} [1 + \mathcal{O}(M/r)],$$

$$C_l \equiv (-2)^{l+1} (2l+1)! / (2l+1)!! , \quad (\text{IV-2})$$

if q_i is the initial multipole moment; (ii) $\Psi(r)$ is well behaved² at the event horizon ($r = 2M$). For the electromagnetic and for the gravitational case, stationary solutions well behaved at the event horizon can be written in terms of hypergeometric functions so that the solutions in equation (IV-1) are

$$\begin{aligned} \tilde{\Psi}_A &= q_i C_l (2M/t)^{2l+2} K_A F(l, -l-1; 1; 1 - r/2M) [1 + \mathcal{O}(1/t)], \\ \tilde{\Psi}_G &= q_i C_l (2M/t)^{2l+2} (2M/r) K_G F(l-1, -l-2; 1; 1 - r/2M) [1 + \mathcal{O}(1/t)], \\ K_A &= \lim_{x \rightarrow \infty} \{x^{l+1}/F(l, -l-1; 1; 1-x)\}, \\ K_G &= \lim_{x \rightarrow \infty} \{x^{l+2}/F(l-1, -l-2; 1; 1-x)\}. \end{aligned} \quad (\text{IV-3})$$

For the electromagnetic dipole the form of equations (IV-3) is particularly simple:

$$\tilde{\Psi}_A = 4q_i (2M/t)^4 (r/2M)^2 [1 + \mathcal{O}(1/t)]. \quad (\text{IV-4})$$

Figure 10a shows the t^{-4} falloff. To check the radial dependence of the tail we plot in Figure 11 the large t value of $t^4 \tilde{\Psi}_A$, for electromagnetic dipole radiation, as a function of r . The computed values show very good agreement with the prediction of equation (IV-4), differing noticeably only at large values of r where the condition $|t/r_*| \gg 1$ is not fulfilled. The disagreement at large r can be viewed as a contamination of the $1/t^4$ tail by a part of the field which falls off more quickly in time. (In fact, if the theoretical prediction of eq. [IV-4] is subtracted from the computed results, the difference falls off as t^{-5} with considerable accuracy.)

b) Quasi-normal Ringing

Normal modes of dynamical systems are motions with time dependence $e^{i\omega t}$ at a real frequency ω . Perturbation fields in a black hole background cannot exhibit such modes (radiation damps any oscillation), but there are

² This is not explicitly stated by Price (1972) but is inherent in his analysis. For instance, the matching of his equations (53) and (56) imply that $\Psi(r) \rightarrow \text{constant}$ at $r \rightarrow 2M$.

FIG. 10.—Electromagnetic and gravitational wave amplitudes as a function of time, showing development of the predicted $t^{-(2l+2)}$ tails. Plots are for collapse from $r_0 = 4M$, with unit initial multipole moment ($q_i/2M = 1$), computed at four values of $r/2M$: (a) 3.1419, (b) 6.2491, (c) 13.3970, and (d) 20.9241. The oscillations appearing in the tail of the gravitational wave function for $r/2M = 3.1419$ are caused by round-off errors in the initial stationary solution and are not of physical significance.

nevertheless special frequencies of interest. If time dependence $e^{i\omega t}$ is assumed in equation (I-1), the result is an ordinary differential equation in r_* , and specification of boundary conditions at $r_* = \pm\infty$ leads to an eigenvalue problem for ω . The boundary conditions of astrophysical relevance are those of ingoing waves at the horizon

$$\left(\tilde{\psi} \xrightarrow{r_* \rightarrow -\infty} e^{i\omega r_*} \right)$$

and outgoing waves at infinity

$$\left(\tilde{\psi} \xrightarrow{r_* \rightarrow +\infty} e^{-i\omega r_*} \right).$$

Quasi-normal frequencies, the solutions to this eigenvalue problem, have been studied by Press (1971), Goebel (1972), and Chandrasekhar and Detweiler (1975).

It should be noted that the boundary conditions on the eigenvalue equation are not of the Sturm-Liouville type and the problem is not self-adjoint. The usual conclusions, then, do not apply. In particular, the eigenvalues ω^2 are not necessarily real and the eigenfunctions are not likely to form a complete set. That ω^2 is not real is intuitively obvious since a mode should represent a damped oscillation.

Quasi-normal frequencies depend on the details of the curvature potential in equation (I-1) and therefore are different for each multipole, and are different for electromagnetic, gravitational, scalar perturbations, etc. The determination of quasi-normal frequencies is hindered by numerical problems, but Chandrasekhar and Detweiler (1975) have found two, three, and four modes for $l = 2, 3, 4$, respectively in the case of the gravitational potential. These are the modes with the least damping, but there may be other modes with greater damping. Studies of analytically tractable model potentials suggest that many highly damped modes may exist (Detweiler 1977).

Quasi-normal modes should be of astrophysical relevance for any process involving dynamical perturbations close to the event horizon. Such perturbations in the region of strong potential should excite quasi-normal ringing of the field and result in radiation to a distant observer (and at the event horizon) exhibiting quasi-normal frequencies. These quasi-normal oscillations should be particularly evident at late times since they are typically more slowly damped than the source exciting them. [On a timelike line which crosses the event horizon, any perturbation field must die off at least as fast as $\exp(-\tilde{u}/4M)$, where \tilde{u} is retarded time (Price 1972), so that quasi-normal frequencies with imaginary parts less than $(4M)^{-1}$ will, at large times, dominate the "direct" outgoing radiation from the perturbing source.] Quasi-normal ringing has been found by Davis, Ruffini, and Tiomno (1972) and by Chung (1973) in the radiation from a particle falling into a black hole, and by Vishveshwara (1970) for waves scattered by a black hole. The question of quasi-normal ringing is discussed in a recent review by Thorne (1978).

Figures 5 show clearly that after an initial burst the fields generated by a perturbed collapse are characterized by damped sinusoidal oscillations. The fact that the frequencies are the same (the nodes align) for different initial radii, and are the same (Fig. 6) for different rates of collapse, demonstrates convincingly that this damped oscillation is not a peculiarity of the excitation but rather a feature of the background spacetime geometry. The frequency and damping rate of these damped oscillations can be read off the graphs and are given in terms of a complex frequency in Table 1. For comparison, the gravitational quasi-normal frequencies found by Chandrasekhar and Detweiler (1975) are also listed. The striking agreement of the observed complex frequencies with the values given by Chandrasekhar and Detweiler (1975) leaves no doubt that quasi-normal ringing is strongly evident in the emerging radiation. Unfortunately no computations of quasi-normal frequencies in the electromagnetic case are available for comparison.

It is tempting to ask whether quasi-normal modes, other than the "fundamental" (least damped) mode, can be seen in the radiation. To search for the second mode in the gravitational quadrupole case we have subtracted, from the numerical data, a term proportional to pure ringing at the fundamental quasi-normal mode, with amplitude

TABLE 1
COMPLEX FREQUENCIES* $2M\omega$

l	Electromagnetic Fields	Gravitational Fields	Quasi-normal Gravitational Frequencies†
1.....	$0.497 \pm 0.008 + (0.190 \pm 0.008)i$		
2.....	$0.914 \pm 0.001 + (0.1892 \pm 0.0003)i$	$(0.7466 \pm 0.0008) + (0.1772 \pm 0.0003)i$	$0.74734 + 0.17792i$ $0.69687 + 0.54938i$
3.....	$1.3112 \pm 0.0003 + (0.1902 \pm 0.0001)i$	$(1.1968 \pm 0.0002) + (0.1843 \pm 0.0001)i$	$1.19889 + 0.18541i$ $1.16402 + 0.56231i$ $0.85257 + 0.74546i$

* Numerical uncertainties stated represent scatter in the frequencies and damping rate of the late-time fields.

† As determined by Chandrasekhar and Detweiler 1975.

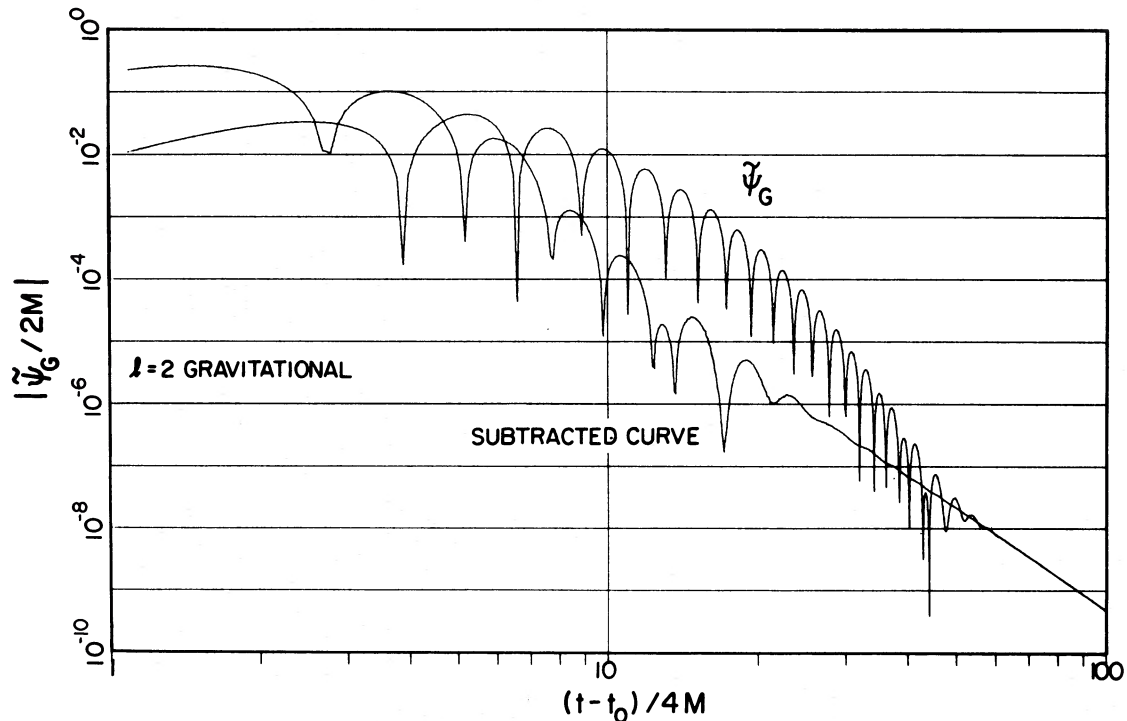


FIG. 12.—Fundamental quasi-normal ringing subtracted from $\tilde{\psi}_G$ for quadrupole gravitational radiation. The subtracted curve represents $\tilde{\psi}_G - A \exp(-\omega_I t) \sin(\omega_R t - \delta)$ where ω_R , ω_I are the real and imaginary parts of the least damped quasi-normal frequency. The parameters A and δ are chosen to minimize oscillations at late times in the subtracted curve.

and phase adjusted to minimize oscillations at late times. The result is plotted in Figure 12. The signature of the second quasi-normal mode $\omega_2 = (0.69687 + 0.54938i)(2M)^{-1}$ is a ratio between the magnitudes of adjacent peaks (maximum and minimum) of

$$\exp \{ \text{Im}(\omega_2) \pi / \text{Re}(\omega_2) \} \approx 12. \quad (\text{IV-5})$$

There is some indication in Figure 12 of the appearance of an oscillation with a damping rate of this order. It should be noted that the last few oscillations in the residual curve must be ignored. These fall near or below the extrapolated t^{-6} tail of the field, and we should expect the tail strongly to contaminate the ringing. The early time region of the curve must also be ignored since it is contaminated by the initial burst of radiation from the collapse.

Figures 5 not only show that quasi-normal ringing appears in the outgoing radiation, but in fact that *quasi-normal ringing seems in some sense to dominate the radiation*. To investigate this quantitatively, we consider in Figure 13 to what extent the quadrupole gravitational spectrum (cf. Fig. 7) for collapse from $r_0 = 8M$ can be approximated by (i) the spectrum of pure quasi-normal ringing at the fundamental quasi-normal frequency, and by (ii) the spectrum of the two Chandrasekhar and Detweiler (1975) quasi-normal modes (cf. Table 1) with relative amplitude and phase adjusted for a good fit to the actual spectrum. The one-mode spectrum gives only a rough approximation, but the two-mode spectrum provides an excellent approximation to the main peak of the spectrum. The fact that the two-mode approximation does not reproduce the small secondary low-frequency peak is consistent with the interpretation that this secondary peak is produced by the initial burst of radiation. A comparison of Figures 7 and 13 shows that the main peak of the spectrum for $r_0 = 20M$ is also very well approximated. The two-mode spectrum, however, does not give as good a fit to the $r_0 = 4M$ collapse, nor can it be improved with a different choice of relative amplitudes and phases; all such two-mode spectra are somewhat broader than the $r_0 = 4M$ spectrum. This is caused by the circumstance that the initial burst of radiation in the $r_0 = 4M$ case falls at about the same frequency as the quasi-normal ringing. (Note the absence of a secondary peak in the $r_0 = 4M$ spectrum in Fig. 7.) To check that the impressive agreement in Figure 13 is not a result of the freedom to choose two parameters (relative phase and amplitude) in superposing two modes we have tried to reproduce the $l = 3$ gravitational spectrum with the same two ($l = 2$) modes and have found it impossible to achieve even a rough agreement.

Although quasi-normal modes account very well for most of the radiation in the above example, we wish to caution against the assumption that quasi-normal ringing generally accounts for nearly all the radiation. That this is not so is made clear if we consider electromagnetic dipole radiation. In this case arguments based on the idealized potential (Price 1972) suggest that the single quasi-normal frequency given in Table 1 is the only quasi-normal

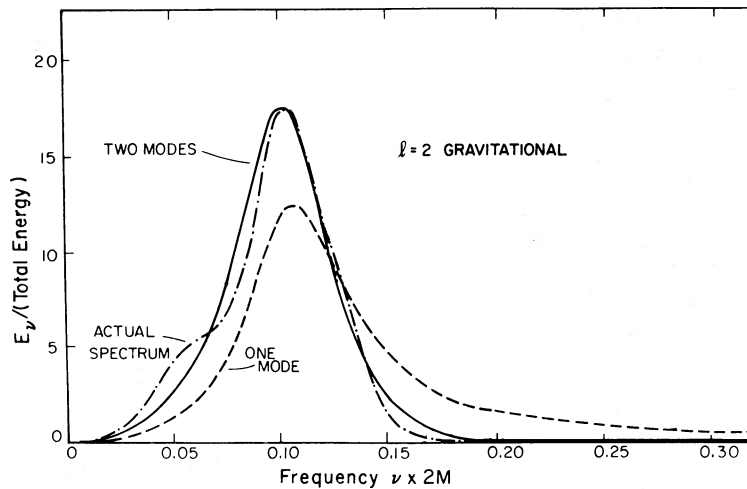


FIG. 13.—Gravitational quadrupole spectrum for collapse from $r_0 = 8M$, compared with spectra for one (ω_1) and for the two quasi-normal modes: $\omega_1 = (0.64734 + 0.17792i)/2M$ and $\omega_2 = (0.69688 + 0.5493i)/2M$. A good fit to the actual spectrum is achieved by the two-mode spectrum plotted,

$$\psi \propto \text{Re} [(1 - 0.3i) \exp(i\omega_1 t) - (1 + 0.5i) \exp(i\omega_2 t)],$$

corresponding to roughly equal excitation of the two modes.

frequency with small damping. We are constrained then to try and fit the dipole spectrum (cf. Fig. 8) with a single mode. The comparison, plotted in Figure 14, is not very satisfactory. Figure 5a also shows that the initial phase, rather than the quasi-normal ringing, probably accounts for most of the energy radiated in the electromagnetic dipole collapses from small radii.

The limitations of quasi-normal modes in representing the field are also inherent in the fact that they do not provide a complete set of basis functions. (It is at least extremely implausible that the quasi-normal modes are complete. For the idealized potential [Price 1972] the modes are clearly an incomplete set since, for any l , there are only a finite number of quasi-normal frequencies.)

There is a reason even more basic why quasi-normal modes will not be dominant in many cases. Oppenheimer-Snyder collapse, or the similar drumhead collapses, have no inherent hydrodynamical or other oscillatory time scales so that there is in some sense very little radiation being generated within the star and passing outward to infinity. The radiation is generated rather by the interaction of the surface and the potential, i.e., by the excitation of the exterior geometry into quasi-normal ringing.

Most astrophysical processes of course do have some inherent time scale, and radiation at frequencies corresponding to that time scale should dominate the spectrum of outgoing radiation. The point we wish to emphasize, however,

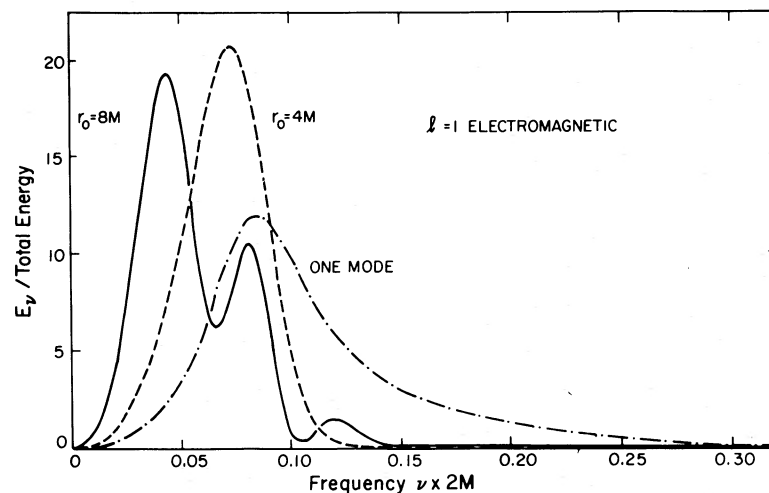


FIG. 14.—Electromagnetic dipole spectrum for initial radii $r_0 = 4M$ and $r_0 = 8M$ compared with the spectrum of the pure $l = 1$ electromagnetic quasi-normal mode.

is that at the late stages of the collapse of an astrophysical object, of a particle falling into a black hole, etc., these time scales are irrelevant. More precisely, the passage from, say, $r = 6M$ to the horizon will occur in a proper time small compared to inherent dynamical time scales. So in the late stages of such processes the radiation generated will not depend on the internal dynamics of the system but rather on the extent to which quasi-normal ringing is excited.

It becomes important, therefore, to be able to estimate the excitation of quasi-normal ringing in an astrophysical collapse. An analysis of quasi-normal ringing in the idealized potential (Price 1972) suggests that the first and largest peak ψ_{peak} of the quasi-normal ringing is related to ψ_s , the field value at the stellar surface, by

$$\psi_{\text{peak}} \approx \left[\left(\frac{dr_*/d\tilde{u}}{dr_*/d\tilde{u} + 1} \right)^l \psi_s \right]_{\text{max. pot.}} \quad (\text{IV-6})$$

Here $r_*(\tilde{u})$ describes the location of the stellar surface as a function of retarded time \tilde{u} . The right-hand side is evaluated near the peak of the potential; evaluation at $r = 4M$ gives good results. The approximation for the surface fields in equation (III-12) and our numerical results then give us

$$\begin{aligned} \psi_{A \text{ peak}} &\approx q_l \left(\frac{r_0}{2M} \right)^{-l} F\left(a, b; c; \frac{2M}{r_0}\right) \left[\left(0.57 \frac{dr_*/d\tilde{u}}{dr_*/d\tilde{u} + 1} \right)^l \right]_{r=4M} \equiv N_A, \\ \psi_{G \text{ peak}} &\approx q_l \left(\frac{r_0}{2M} \right)^{-l} \left(\frac{r_0}{4M} \right) F\left(a, b; c; \frac{2M}{r_0}\right) \left[\left(0.57 \frac{dr_*/d\tilde{u}}{dr_*/d\tilde{u} + 1} \right)^l \right]_{r=4M} \equiv N_G, \end{aligned} \quad (\text{IV-7})$$

where F is the hypergeometric function defined in equation (III-6).

If the radiation is dominated by quasi-normal ringing, then the total radiation energy E emitted in a given multipole mode should depend only on the magnitude of the peak of the quasi-normal ringing. Assuming that little energy is radiated before this peak and that the least damped mode, of complex frequency ω , is dominant thereafter, our approximation in equation (IV-7) suggests

$$E \approx \frac{1}{4} \kappa \frac{|\omega|^2}{\text{Im}(\omega)} N^2, \quad (\text{IV-8})$$

where κ , given in equation (III-25), depends upon l and on whether the perturbation is electromagnetic or gravitational.

This approximation for the energy is compared to numerical values in Figure 9. As might be expected, the approximation is rather good for large values of r_0 , but fails for stars with initial radii near that of the potential maximum.

We shall discuss elsewhere in greater detail the problem of estimating quasi-normal excitation and the relevance of quasi-normal radiation to astrophysical processes.

Equation (IV-8) allows us to estimate the maximum energy that can be radiated during the collapse of our models from large radii ($r_0 \gg M$). Near $\chi = 0$, regularity demands that $U(\chi) \propto (\sin \chi)^{l+1}$. For $r_0 \gg 2M$ we have $2M/r_0 = \sin^2 \chi_0 \approx \chi_0^2 \ll 1$, and we take for $U(\chi)$

$$U(\chi) = U_0 (\sin \chi / \sin \chi_0)^{l+1} \approx U_0 (\chi / \chi_0)^{l+1}, \quad (\text{IV-9})$$

where $U_0 = U(\chi_0)$ is a constant. With this form of the source we can calculate the magnitude of the multipole moment it produces (cf. Appendix B); using the "Newtonian" approximation of Appendix B, we find that

$$q_l = -\frac{6l(l+1)(l+2)U_0}{(2l+1)(2l+3)} \left(\frac{r_0}{2M} \right)^{l-1}. \quad (\text{IV-10})$$

An upper limit for q_l now follows from the requirement that there be no centrifugal shedding. A particle freely falling in a bounded orbit in the Schwarzschild geometry can fall through the event horizon only if U_ϕ , its angular momentum per unit mass, satisfies

$$U_\phi \leq 4M \quad (\text{IV-11})$$

(Misner, Thorne, and Wheeler 1973, pp. 660–662). Particles with larger angular momentum will reach a periastron outside the horizon. Since the fluid particles at the surface of our models are freely falling in the (approximately) Schwarzschild exterior, equation (IV-11) gives a natural upper limit on the angular momentum per unit mass of these particles:

$$|U_\phi|_{\chi_0} = |U(\chi_0) \sin \theta \partial Y_{l0} / \partial \theta| \leq 4M. \quad (\text{IV-12})$$

A more rapidly rotating model would presumably disrupt before all of its matter passed through the event horizon. Such disrupting models may indeed radiate more energy than our slowly rotating models, but they would not be amenable to a purely perturbative calculation.

For simplicity we consider only the dominant quadrupole ($l = 2$) radiation and find, after calculating the maximum of the angular factor $\sin \theta \partial Y_{10} / \partial \theta$, that equation (IV-12) requires

$$|U_0| = |U(\chi_0)| \leq 2M(12\pi/5)^{1/2} \quad (\text{IV-13})$$

and (eq. [IV-10])

$$q_2 \leq (144/35)(12\pi/5)^{1/2} r_0. \quad (\text{IV-14})$$

For $r_0/2M \gg 1$ the factor involving $dr_*/d\tilde{u}$ in equation (IV-7) is easily evaluated from $(dr/d\tau)^2 \approx 2M/r$, and equations (IV-8) and (IV-14) give the upper limit for the radiated energy E_{max} . It is interesting to note that (for any $l \geq 2$) the upper limit estimates E_{max}/M approach a constant as $2M/r_0 \rightarrow 0$. For $l = 2$ it has the approximate value

$$E_{\text{max}} \xrightarrow{r_0 \rightarrow \infty} 1.2 \times 10^{-3} M. \quad (\text{IV-15})$$

We reiterate that this estimate applies only to the odd-parity "slowly rotating" models considered here, and makes use of a special form (eq. [IV-9]) of the source function $U(\chi)$.

We wish to thank Steven Detweiler and Kip S. Thorne for useful discussions of quasi-normal modes. We wish also to thank Anthony Hearn, Martin Griss, and Cedric Griss, of the Computational Physics group at the University of Utah, for their help in using the symbolic manipulation language REDUCE to derive the perturbation equations for the stellar interior.

APPENDIX A

JUNCTION CONDITIONS

The derivation of the junction conditions at the boundary surface is facilitated if we introduce Novikov (1963) coordinates $(\tau, R^*, \theta, \phi)$ in the exterior region. In these coordinates the exterior line element is

$$ds^2 = -d\tau^2 + \left(\frac{R^{*2} + 1}{R^{*2}} \right) \left(\frac{\partial r}{\partial R^*} \right)^2 dR^{*2} + r^2(d\theta^2 + \sin^2 \theta d\phi^2), \quad (\text{A1})$$

where

$$\begin{aligned} r &= M(R^{*2} + 1)(1 + \cos \eta), \\ \tau &= M(R^{*2} + 1)^{3/2}(\eta + \sin \eta); \end{aligned} \quad (\text{A2})$$

and in this system the unperturbed boundary surface is simply

$$R^* = R_0^* = \cos \chi_0 / \sin \chi_0, \quad \sin \chi_0 = (R_0^{*2} + 1)^{-1/2}. \quad (\text{A3})$$

We can always require, with a suitable choice of coordinates, that the boundary surfaces of the perturbed spacetime have the same fixed coordinate characterization. The surfaces labeled $\chi = \chi_0$ (interior) and $R^* = R_0^*$ (exterior) may be identified with one another as the perturbed star's boundary provided (i) the perturbed fluid velocity is tangent to the surface and (ii) the perturbed first and second fundamental forms are continuous at the surface. For first (n th) order perturbations each condition must be satisfied up to first (n th) order in the perturbation parameter ϵ .

Condition (i) is trivially satisfied for first-order odd-parity perturbations since the unperturbed fluid velocity is $U^\mu = \delta^\mu_\tau$ and its first-order perturbation obeys

$$\left. \frac{\partial U^\chi}{\partial \epsilon} \right|_{\epsilon=0} = -\frac{1}{R^2} h_{\chi\tau} + \frac{1}{R^2} \left. \frac{\partial U_\chi}{\partial \epsilon} \right|_{\epsilon=0} \equiv 0 \quad (\text{A4})$$

(since $h_{\chi\tau} = \partial U_\chi / \partial \epsilon|_{\epsilon=0} \equiv 0$ for odd-parity perturbations).

To impose condition (ii) we express the exterior perturbations in Novikov coordinates $(\tau, R^*, \theta, \phi)$. The match conditions are then simply

$$\begin{aligned} h_{ab}|_{\chi_0} &= \tilde{h}_{ab}|_{R_0^*}, \\ \frac{\partial}{\partial \epsilon} [(g^{xx})^{-1/2} \Gamma_{ab}^x]|_{\epsilon=0, x=\chi_0} &= \frac{\partial}{\partial \epsilon} [(\tilde{g}^{R^*R^*})^{-1/2} \tilde{\Gamma}_{ab}^{R^*}]|_{\epsilon=0, R^*=R_0^*}, \end{aligned} \quad (\text{A5})$$

where Γ_{ab}^x and $\tilde{\Gamma}_{ab}^{R^*}$ are Christoffel symbols of the interior and exterior metrics and where a, b range over (τ, θ, ϕ) the (continuous) coordinate functions on the boundary surface.

A straightforward computation (using the transformation from Schwarzschild to Novikov coordinates in the exterior) yields from equations (A5):

$$\begin{aligned}
 h_0|_{x_0} &= \left\{ \frac{R^*(R^{*2} + 1)^{1/2}(1 + \cos \eta)^2 \tilde{h}_0}{[(R^*)^2(1 + \cos \eta)^2 - \sin^2 \eta]} - \frac{\sin \eta \tilde{h}_1}{(R^{*2} + 1)^{1/2}(1 + \cos \eta)} \right\} \Big|_{R_0^*}, \\
 h_2|_{x_0} &= \tilde{h}_2|_{R_0^*}, \\
 \left[\frac{\cos \chi}{R} \left(q_1 + \frac{h_2}{\sin \chi} \right) \right] \Big|_{x_0} &= \left[\frac{\tilde{h}_2 R^*}{r(R^{*2} + 1)^{1/2}} - \frac{\partial(r^2 \tilde{\pi}_1)/\partial \tau}{l(l+1)(l-1)(l+2)} \right] \Big|_{R_0^*}, \\
 \frac{\pi_1}{l(l+1)} \Big|_{x_0} &\equiv \left\{ R \cos \chi \frac{\partial}{\partial \tau} \left(\frac{q_1}{R^2} \right) - \frac{R \sin^2 \chi}{2} \frac{\partial}{\partial \chi} \left[\frac{1}{\sin^2 \chi} \frac{\partial}{\partial \tau} \left(\frac{q_2}{R^2} \right) + \frac{2h_0}{R^2 \sin^2 \chi} \right] \right\} \Big|_{x_0} = \frac{\tilde{\pi}_1}{l(l+1)} \Big|_{R_0^*}, \quad (\text{A6})
 \end{aligned}$$

where we have used the exterior field equations given by Moncrief (1974) to reexpress the (Schwarzschild) time derivatives of q_1 , etc., in terms of π_1 , etc. From these same exterior equations one can also derive

$$\begin{aligned}
 &\frac{-2(r\tilde{\pi}_1)_{,R^*}}{l(l+1)(l-1)(l+2)} \left[\frac{R^*(1 + \cos \eta)^2}{2(1 + \cos \eta)^2 + 3 \sin \eta(\eta + \sin \eta)} \right] \\
 &= \frac{R^* r^2}{(R^{*2} + 1)^{1/2}} \frac{\partial}{\partial \tau} \left(\frac{\tilde{h}_2}{r^2} \right) + \frac{2(r\tilde{\pi}_1)}{l(l+1)(l-1)(l+2)} \frac{(R^*)^2}{(R^{*2} + 1)} \\
 &+ \frac{2R^*}{(R^{*2} + 1)^{1/2}} \left[\frac{R^*(R^{*2} + 1)^{1/2}(1 + \cos \eta)^2 \tilde{h}_0}{R^{*2}(1 + \cos \eta)^2 - \sin^2 \eta} - \frac{\sin \eta \tilde{h}_1}{(R^{*2} + 1)^{1/2}(1 + \cos \eta)} \right]. \quad (\text{A7})
 \end{aligned}$$

From equations (A6) it is evident that, at the boundary surface, each term on the right-hand side of equations (A7) may be equated with the boundary value of an interior function (e.g., π_1 , h_0 , h_2) with the possible exception of $\tilde{h}_{2,\tau}$. However, since $h_2 = \tilde{h}_2$ at the boundary, and since $\partial/\partial \tau|_{R^*}$ is a derivative tangent to the boundary, we may equate

$$h_{2,\tau}|_{x_0} = \tilde{h}_{2,\tau}|_{R_0^*}. \quad (\text{A8})$$

Finally $h_{2,\tau} \equiv q_{2,\tau}$ (cf. eq. [II-3b]) can be reexpressed through the use of equation (II-8c) to yield the matching equation

$$\tilde{n}^\mu \tilde{\pi}_{1,\mu}|_{R_0^*} = [n^\mu \pi_{1,\mu} + l(l+1)16\pi\rho U]|_{x_0}. \quad (\text{A9})$$

Equations (A6) and (A9) provide the fundamental matching conditions used in § II.

APPENDIX B

INITIAL DATA AND MULTIPOLE MOMENTS

We here solve the gravitational initial data problem formulated in § II for an arbitrary (regular) source function $U(\chi)$. Setting $\pi_1|_{\text{hom}} = 0$ on the initial ($t = \tau = 0$) surface, we must find the solution $C(\chi) = R^2 \pi_1$ of

$$\frac{1}{\sin^2 \chi} \frac{d}{d\chi} \left[\sin^2 \chi \frac{dC}{d\chi} \right] - \frac{l(l+1)}{\sin^2 \chi} C = -16\pi\rho R^3 U_{,\chi} l(l+1) \quad (\text{B1})$$

which matches smoothly to the stationary solution of the RW equation which is well behaved at $r = \infty$.

Let $C_{\text{reg}}(\chi)$ and $C_{\text{irr}}(\chi)$ be the solutions of the homogeneous form of equation (B1) which behave, respectively, as

$$\begin{aligned}
 C_{\text{reg}}(\chi) &\xrightarrow{\chi \rightarrow 0} \chi^l, \\
 C_{\text{irr}}(\chi) &\xrightarrow{\chi \rightarrow 0} \chi^{-(l+1)}. \quad (\text{B2})
 \end{aligned}$$

Then, any solution of equation (B1) which is regular at $\chi = 0$ has the form

$$C(\chi) = \gamma C_{\text{reg}}(\chi) + \int_0^{\chi_0} d\chi' \{ G(\chi, \chi') \sin^2 \chi' [-16\pi\rho R^3 U_{,\chi'} l(l+1)] \}, \quad (\text{B3})$$

where γ is a constant, and where the Green's function $G(\chi, \chi')$ is given by

$$\begin{aligned} G(\chi, \chi') &= \frac{C_{\text{irr}}(\chi')C_{\text{reg}}(\chi)}{\sin^2 \chi' W(\chi')} \quad \text{if } \chi \leq \chi' \\ &= \frac{C_{\text{reg}}(\chi')C_{\text{irr}}(\chi)}{\sin^2 \chi' W(\chi')} \quad \text{if } \chi \geq \chi', \end{aligned} \quad (\text{B4})$$

in which the Wronskian

$$W(\chi) \equiv [C_{\text{reg}}(\chi)dC_{\text{irr}}(\chi)/d\chi - C_{\text{irr}}(\chi)dC_{\text{reg}}(\chi)/d\chi] \quad (\text{B5})$$

satisfies

$$\sin^2 \chi W(\chi) = \text{constant} \neq 0. \quad (\text{B6})$$

We must match this solution to the exterior stationary solution

$$r\tilde{\pi}_1 = \tilde{\psi}_G \equiv q_l r \tilde{\Lambda} \quad (\text{B7})$$

of the RW equation which has the asymptotic form

$$r\tilde{\pi}_1 \xrightarrow{\tau \rightarrow \infty} q_l (2M/r)^l \quad (\text{B8})$$

or

$$\tilde{\Lambda} \xrightarrow{\tau \rightarrow \infty} (1/r)(2M/r)^l. \quad (\text{B9})$$

Putting

$$Q_l \equiv - \int_0^{\chi_0} d\chi' \{ \sin^2 \chi' C_{\text{reg}}(\chi') [16\pi\rho R^3 U_{,x} l(l+1)] \}, \quad (\text{B10})$$

we can write the initial matching conditions (eqs. [II-17] with $\tau = t = 0$, and with $\pi_1|_{\text{hom}} = 0$ in eq. [II-19]) as

$$\begin{aligned} \gamma C_{\text{reg}}(\chi_0) - q_l R^2(0) \tilde{\Lambda}(r_0) &= - \left[\frac{C_{\text{irr}}(\chi_0)}{\sin^2 \chi_0 W(\chi_0)} \right] Q_l, \\ \gamma \frac{d}{d\chi} C_{\text{reg}}(\chi_0) - R^2(0) \left(1 - \frac{2M}{r_0} \right)^{1/2} \tilde{\Lambda}_{,r}(r_0) q_l &= - \left\{ \left[\frac{dC_{\text{irr}}(\chi_0)/d\chi}{\sin^2 \chi_0 W(\chi_0)} \right] Q_l + 16\pi\rho R^3 U(\chi_0) l(l+1) \right\}. \end{aligned} \quad (\text{B11})$$

These are linear, inhomogeneous equations for the two constants γ and q_l which are thereby determined once the sources are specified.

The solution for q_l can be written

$$\begin{aligned} q_l [\sin^2 \chi_0 R^2(0) (1 - 2M/r_0)^{1/2} \tilde{\Lambda}_{,r}(r_0) C_{\text{reg}}(\chi_0) - \sin^2 \chi_0 R^2(0) \tilde{\Lambda}(r_0) dC_{\text{reg}}(\chi_0)/d\chi] \\ = \int_0^{\chi_0} d\chi' \{ 16\pi\rho R^3 U(\chi') l(l+1) d[\sin^2 \chi' C_{\text{reg}}(\chi')]/d\chi' \}, \end{aligned} \quad (\text{B12})$$

where the contribution proportional to $U(\chi_0)$ has been canceled by the surface term resulting from an integration by parts.

Recalling that

$$(4\pi/3)\rho(0)r_0^3 = M, \quad R^2(0) = r_0^3/2M, \quad 16\pi\rho R^3 = 6r_0(r_0/2M)^{1/2}, \quad (\text{B13})$$

we can rewrite this result as

$$\begin{aligned} q_l \left[r_0^2 \left(\frac{r_0}{2M} \right)^{1/2} \left(1 - \frac{2M}{r_0} \right)^{1/2} \tilde{\Lambda}_{,r}(r_0) C_{\text{reg}}(\chi_0) - r_0 \tilde{\Lambda}(r_0) \frac{d}{d\chi} C_{\text{reg}}(\chi_0) \right] \\ = 6l(l+1) \left(\frac{r_0}{2M} \right)^{1/2} \int_0^{\chi_0} d\chi' \left\{ U(\chi') \frac{d}{d\chi'} [\sin^2 \chi' C_{\text{reg}}(\chi')] \right\}, \end{aligned} \quad (\text{B14})$$

where χ_0 and r_0 are related by

$$\sin^2 \chi_0 = 2M/r_0. \quad (\text{B15})$$

The regularity condition on $U(\chi)$ at $\chi = 0$ is determined by the requirement that

$$X^\mu \delta U_\mu = U(\chi) \sin \theta \partial Y_{10} / \partial \theta \quad (\text{B16})$$

be a regular function of locally Cartesian coordinates at the center ($\chi = 0$) of the star. (Here $X^\mu \partial_\mu = \partial/\partial\phi$ is the Killing field of azimuthal symmetry.) From the specified angular dependence it is straightforward to show that this condition requires

$$U(\chi) \xrightarrow{\chi \rightarrow 0} \text{const.} \times (\sin \chi)^{l+1}. \quad (\text{B17})$$

The solutions C_{irr} may be written as

$$C_{\text{irr}}(\chi) = (\sin \chi)^{-(l+1)} \Phi_l(\cos \chi) \quad (\text{B18})$$

where Φ_l is related to Gegenbauer polynomials (Abramowitz and Stegun 1965) and is given by the Rodrigues formula

$$\Phi_l(\xi) = (1 - \xi^2)^{l+1/2} \left(\frac{d}{d\xi} \right)^{l+1} (1 - \xi^2)^{1/2}. \quad (\text{B19})$$

The solution well behaved at $\chi = 0$ may then be found from $C_{\text{irr}}(\chi)$ as

$$C_{\text{reg}}(\chi) = C_{\text{irr}}(\chi) \int_0^\chi [\sin \chi' C_{\text{irr}}(\chi')]^{-2} d\chi'. \quad (\text{B20})$$

The integrals arising in equation (B20) can always be evaluated in closed form. For the quadrupole ($l = 2$) case the functions are

$$\begin{aligned} C_{\text{irr}}(\chi) &= -3 \cos \chi / \sin^3 \chi, \\ C_{\text{reg}}(\chi) &= \frac{\sin^3 \chi - 3 \sin \chi + 3\chi \cos \chi}{6 \sin^3 \chi}. \end{aligned} \quad (\text{B21})$$

If $r_0 \gg 2M$ (i.e., if the initial radius is much larger than the Schwarzschild radius), then $\chi_0 \ll 1$ and for any $l \geq 2$ we may use the approximations

$$\begin{aligned} C_{\text{reg}}(\chi) &\approx \sin^l \chi \approx \chi^l, \\ C_{\text{irr}}(\chi) &\approx (\sin \chi)^{-l-1} \approx \chi^{-l-1}. \end{aligned} \quad (\text{B22})$$

These ‘‘Newtonian’’ approximations ignore the spatial curvature of the initial hypersurface.

The problem of justifying the choice $a_{\text{hom}} = 0$ (see eq. [II-35]), and of relating an electromagnetic multipole moment q_l to the source current, is solved similarly.

REFERENCES

- Abramowitz, M., and Stegun, I. A. 1965, *Handbook of Mathematical Functions* (New York: Dover), chap. 22.
- Chandrasekhar, S., and Detweiler, S. 1975, *Proc. Roy. Soc. London*, **344**, 441.
- Chung, K. P. 1973, *Nuovo Cimento*, **14B**, 293.
- Davis, M., Ruffini, R., and Tiomno, J. 1972, *Phys. Rev. D*, **5**, 2932.
- Detweiler, S. 1977, private communication.
- Goebel, C. J. 1972, *Ap. J. (Letters)*, **172**, L95.
- Landau, L. D., and Lifshitz, E. M. 1975, *The Classical Theory of Fields* (4th ed.; London: Pergamon), eq. [107.12].
- Lifshitz, E. M., and Khalatnikov, I. M. 1963, *Adv. Phys.*, **12**, 185.
- Misner, C. W., Thorne, K. S., and Wheeler, J. A. 1973, *Gravitation* (San Francisco: Freeman).
- Møller, C. 1952, *The Theory of Relativity* (New York: Academic Press).
- Moncrief, V. 1974, *Ann. Phys.*, **88**, 323.
- Novikov, I. D. 1963, doctoral dissertation, Shternberg Astronomical Institute, Moscow. See also Misner, Thorne, and Wheeler (1973), §31.4.
- Oppenheimer, J. R., and Snyder, H. 1939, *Phys. Rev.*, **56**, 455.
- Press, W. H. 1971, *Ap. J. (Letters)*, **170**, L105.
- Price, R. H. 1972, *Phys. Rev. D*, **5**, 2419.
- Regge, T., and Wheeler, J. A. 1957, *Phys. Rev.*, **108**, 1063 (RW).
- Sengupta, U. K. 1975, Ph.D. thesis, Ohio State University.
- Thorne, K. S. 1978, in *Theoretical Principles in Astrophysics and Relativity*, ed. N. Lebovitz, W. H. Reid, and P. O. Vandervoort (Chicago: University of Chicago Press).
- Vishveshwara, C. V. 1970, *Nature*, **227**, 936.

CHRISTOPHER T. CUNNINGHAM and RICHARD H. PRICE: Department of Physics, University of Utah, Salt Lake City, UT 84112

VINCENT MONCRIEF: Department of Physics, Yale University, New Haven, CT 06520